A VgrG2b fragment cleaved by caspase-11/4 promotes *Pseudomonas aeruginosa* infection through suppressing the NLRP3 inflammasome

Yan Qian[1,2,3,5], Qiannv Liu[1,2,3,5], Weitao Li[1,2,3], Chunlei Wang[1,2,3], Chun Kong[1,2,3], Mengqian Li[1,2,3], Shuo Wang[4], Pengyan Xia[1,2,3*]

[1]Department of Immunology, School of Basic Medical Sciences, Peking University, Beijing, 100191, China

[2]NHC Key Laboratory of Medical Immunology, Peking University, Beijing, 100191, China

[3]Key Laboratory of Molecular Immunology, Chinese Academy of Medical Sciences, Beijing, 100191, China

[4]CAS Key Laboratory of Pathogen Microbiology and Immunology, Institute of Microbiology, Chinese Academy of Sciences, 100101 Beijing, China

[*]Address correspondence and reprint requests to Dr. Pengyan Xia, Department of Immunology, School of Basic Medical Sciences, Peking University, Beijing, 100191, China, Tel: 86-10-82805759; E-mail: xiap@pku.edu.cn

[5]These authors contributed equally to this work.

Running title: Caspase-11 cleaves VgrG2b to inhibit the NLRP3 inflammasome.

Abstract

The T6SS of *Pseudomonas aeruginosa* plays an essential role in the establishment of chronic infections. Inflammatory cytokines mediated by inflammasomes are crucial for the body to resist bacterial infections. Here we found that during the infection of *P. aeruginosa*, non-canonical inflammasome was activated in macrophages, but the activation of downstream NLRP3 inflammasome was inhibited. The VgrG2b of *P. aeruginosa* is recognized and cleaved by caspase-11, generating a free C-terminal fragment. The VgrG2b C-terminus can bind to NLRP3, inhibiting the activation of the NLRP3 inflammasome by rejecting NEK7 binding to NLRP3. Administrating a specific peptide that inhibits the cleavage of VgrG2b by caspase-11 to mice can significantly improve their survival rate during infection. Our discovery elucidates a mechanism by which *P. aeruginosa* inhibits host immune response, providing a new approach for the future clinical treatment of *P. aeruginosa* infections.

Key words: *P. aeruginosa*; non-canonical inflammasome; caspase-11/4; VgrG2b; NLRP3.

Introduction

Non-canonical inflammasomes are composed of caspase-11 from mice or caspase-4/5 from humans, which can recognize bacteria lipopolysaccharides (LPS) in the cytoplasm[1-3]. Once activated, non-canonical inflammasomes induce the maturation of gasdermin D (GSDMD) to form pores on cell and mitochondrial membranes[4-6]. It also activates the NOD-, LRR- and pyrin domain-containing protein 3 (NLRP3) inflammasome[5,7]. NLRP3 is an important intracellular receptor that can respond to various endogenous and exogenous stimulus signals[8,9]. NLRP3 recruits NIMA-related kinase 7 (NEK7) and undergoes polymerization, inducing the activation of caspase-1 and maturation of interleukin-1β (IL-1β)[8,10]. Non-canonical inflammasomes promote the assembly and final activation of the NLRP3 inflammasome through activating the nuclear orphan receptor NUR77 with the help of LPS and mitochondrial dsDNA[11].

Pseudomonas aeruginosa is an opportunistic pathogenic bacterium widely distributed in the environment, which can cause acute and chronic infections in humans[12,13]. *P. aeruginosa* has multiple secretion systems that are used to secrete virulence factors to the external environment or host cells to promote its survival and infection[13]. Among them, the type III secretion system (T3SS) and the type VI secretion system (T6SS) are two important secretion systems that play important roles in acute and chronic infections of *P. aeruginosa*, respectively[14,15]. T3SS can directly inject effector proteins into target cells to alter their function or cause target cell death[16,17]. *P. aeruginosa* encodes three different T6SSs, namely Hcp secretion island-I (H1)-T6SS, H2-T6SS, and H3-T6SS[18,19]. These T6SSs play a crucial role in biofilm formation, competition between bacteria, and toxicity to host cells[20,21]. H1-T6SS only targets bacteria and is used for competition between bacteria[22]. H2-T6SS and H3-T6SS are involved in interactions between bacteria and host cells[23,24].

The effector proteins of H2-T6SS can target both bacteria and eukaryotic cells[21,23]. T6SS is composed of structural proteins and virulence factors[21,25]. Structural proteins such as hemolysin-coregulated protein (Hcp), valine-glycine repeat protein G (VgrG), and proline-alanine-alanine-arginine repeats (PAAR) form a stable spike-like structure[26,27]. Toxic factors are transported to the extracellular space through T6SS, thereby exerting

toxic effects on other bacteria or host cells[17,21]. VgrG2b is an important component of T6SS, which usually binds tightly to other components of T6SS such as the Hcp protein, together forming the core component of the secretion system[28]. The VgrG2b protein has a special structure for recognizing and binding effector proteins, which are transported to the tip of the secretion system and injected into the target cells[25,28]. VgrG2b entering eukaryotic cells can also regulate the biological functions of host cells through binding to cytoskeletal proteins[28,29].

Here we found that *P. aeruginosa* infection activates caspase-11 but inhibits the activation of NLRP3 inflammasomes in macrophages. The VgrG2b entering the host cell is recognized and cleaved by caspase-11 to generate a free C-terminal fragment. This fragment can bind to NLRP3 and inhibit its binding to NEK7, thereby preventing the activation of the NLRP3 inflammasome. The inhibitory effect of *P. aeruginosa* effectively avoids further activation of the host immune system and plays a crucial role in establishing bacterial infection. Our findings may provide a new perspective for the treatment of *P. aeruginosa* infections in the future.

Results

P. aeruginosa causes abnormal signaling of non-canonical inflammasome

Non-canonical inflammasomes are activated during the infection of Gram-negative bacteria such as *P. aeruginosa in vivo*[2,7,30]. Obstruction of the inflammasome pathway can lead to chronic infections[31,32]. To investigate whether T6SS of *P. aeruginosa* modulated the non-canonical inflammasome pathway to establish chronic infections, we used an *RetS* mutant strain that specifically expresses T6SS[14,33,34]. As an extracellular bacterial, *P. aeruginosa* synthesizes outer membrane vesicles (OMV) to induce non-canonical inflammasome activation[35]. We therefore added *P. aeruginosa* and OMVs to macrophages *in vitro* to simulate the real situation of infection *in vivo* as much as possible[36]. We found that activation of caspase-11 and cleavage of GSDMD in BMDM cells were not affected after incubation with *P. aeruginosa* and OMVs (Fig. 1A, B). However, activation of caspase-1 was significantly inhibited in cells infected with *P. aeruginosa* (Fig. 1A). Consistent with the results of immunoblotting, the secretion of IL-1β was diminished after infection with *P. aeruginosa* (Fig. 1C). Although the mortality rate of *P.*

aeruginosa-infected cells was increased (Fig. 1D) and the survival rate was decreased (Fig. 1E), there was not much difference compared to cells stimulated with intracellular *E. coli*. These results indicate that the activation of NLRP3 inflammasomes post non-canonical inflammasome stimulation is inhibited in the presence of *P. aeruginosa*. Similar results were observed in human macrophage experiments, with normal caspase-4 activation and GSDMD cleavage after *P. aeruginosa* infection (Fig. S1A, B). However, the activation of caspase-1 was suppressed and IL-1β could not be secreted normally in these cells (Fig. S1A, C). *P. aeruginosa* infection, the cell mortality rate was increased (Fig. S1D) and the survival rate was decreased (Fig. S1E), showing no much difference with cells treated only with intracellular *E. coli*.

There might be two mechanisms by which NLRP3 inflammasomes were inhibited during this process. One was that the NLRP3 inflammasome lacked necessary stimuli for activation, and the other was that the NLRP3 inflammasome was inhibited by a bacterial substance. The release of mitochondrial DNA into the cytoplasm is a prerequisite for NLRP3 activation in the non-canonical inflammasome pathway. We first detected the localization of GSDMD N-terminus on the mitochondrial membrane during *P. aeruginosa* infection. The results indicate that GSDMD-N can be normally localized on the mitochondrial membrane (Fig. 1F). In addition, the release of mitochondrial DNA into the cytoplasm was not affected by *P. aeruginosa* infection (Fig. S1F). The binding of NUR77 and NLRP3 was not affected during the infection of *P. aeruginosa* (Fig. S1G). However, the binding of NLRP3 to NEK7 was significantly inhibited (Fig. S1H). These data suggest that the inhibition of NLRP3 is potentially influenced by a certain inhibitory factor from *P. aeruginosa*.

To verify this, we introduced LPS and mitochondrial DNA into macrophages to induce NLRP3 inflammasome activation, bypassing the caspase-11-GSDMD prerequisite[11]. To avoid the activation of the AIM2 inflammasome by mitochondrial DNA, we conducted the following experiments under an *Aim2* knockout background. We found that after introducing LPS and mitochondrial DNA, NLRP3 inflammasomes were activated (Fig. 1G). However, NLRP3 activation was inhibited (Fig. 1G) and the secretion of IL-1β was tremendously inhibited (Fig. 1H) after incubation with *P. aeruginosa*. The

percentage of cells undergoing pyroptosis (Fig. 1I) and the cell viability (Fig. 1J) did not change due to infection with *P. aeruginosa*. This was consistent with previous reports suggesting that GSDMD cleavage by caspase-11, rather than subsequent GSDMD cleavage by NLRP3, is the main factor causing cell death[37,38]. Next, we used *Gsdmd* and *Aim2* double knockout cells to detect the effect of *P. aeruginosa* on NLRP3 inflammasome activation. We found that after *Gsdmd* knockout, the NLRP3 inflammasome became active when LPS and mitochondrial DNA were introduced into macrophages. However, NLRP3 was still inhibited after incubation with *P. aeruginosa* (Fig. S1I). The secretion of IL-1β was also inhibited due to *Gsdmd* deficiency (Fig. S1J). The cell death rate was low due to the absence of GSDMD (Fig. S1K), while the percentage of viable cells was relatively high (Fig. S1L). These results suggest that potent inhibitory factors of *P. aeruginosa* may act upstream of GSDMD. Therefore, we conducted infection experiments using *Casp11* and *Aim2* double knockout cells. After incubation with *P. aeruginosa*, the activation of NLRP3 inflammasome was not affected (Fig. 1K). The secretion of IL-1β was no longer inhibited (Fig. 1L). And the cell death rate was high due to the processing of GSDMD by activated caspase-1 (Fig. 1M), while the survival rate was low (Fig. 1N). These data indicate that the inhibitory factors of *P. aeruginosa* requires caspase-11 to take effect.

Caspase-11 cleaves VgrG2b of *P. aeruginosa*

In order to search for potential substrates of caspase-11 in *P. aeruginosa*, we designed a systematic screening system (Fig. 2A). Simply, we constructed two fluorescent plasmids, one containing green fluorescent protein (GFP), polyclonal sites, and mitochondrial outer membrane localization signals, and the other containing red fluorescent protein (RFP) and mitochondrial outer membrane localization signals. We extracted the mRNA of *P. aeruginosa* and prepared it into a library for insertion into GFP containing plasmids. We co-transfected it with the RFP plasmid into HEK293T cells and sorted the monoclonal cells containing both RFP and GFP signals into a 96-well plate using flow cytometry. Subsequently, the plasmid encoding caspase-11 was transfected into cells, and cells with disappearance of green signal on mitochondria were selected. The target proteins in these cells were cleaved by caspase-11, causing the detachment of

GFP from mitochondria. After sequencing, we found that VgrG1a and VgrG2b repeatedly appeared in cells that met the screening criteria.

We cloned the genes of VgrG1a and VgrG2b and cleaved them using mouse caspase-11. We found that they can both be cleaved (Fig. S2A and Fig. 2B). We also found that they can be cleaved by human caspase-4 (Fig. S2B and Fig. 2C), but not by caspase-11/4 mutants lacking enzymatic activities. These results indicate that our screening system is reliable. The number of target genes screened was very limited, which was consistent with the particularly narrow substrate spectrum of caspae-11[39]. We also tested other members of the VgrG family and found that neither mouse caspase-11 nor human caspase-4 could cleave these members (Fig. S2C–L). VgrG1a and VgrG2b belong to the secretion systems of H1-T6SS and H2-T6SS, and H1-T6SS does not have an effect on eukaryotic cells[22,28]. Therefore, our subsequent research focused on VgrG2b.

Our next concern was whether VgrG2b entered macrophages. We found that after co-culturing of *P. aeruginosa* with BMDM cells, the VgrG2b protein appeared in macrophages (Fig. 2D). Immunofluorescence experiments also showed the presence of bacterial proteins in macrophages after co-incubation with *P. aeruginosa* (Fig. 2E). We then incubated *P. aeruginosa* with wild-type BMDM cells and found that VgrG2b was cleaved in macrophages, while the cleavage band of VgrG2b disappeared in *Casp11*$^{-/-}$ BMDM cells (Fig. 2F). We restored caspase-11 expression in *Casp11*$^{-/-}$ BMDM cells and found that the presence of caspase-11 induced VgrG2b cleavage (Fig. 2G). We also rescued *Casp11*$^{-/-}$ BMDM cells with wild-type and enzymatic mutant caspase-11 and found that mutant caspase-11 could not induce VgrG2b cleavage (Fig. 2H). In addition, we incubated human macrophages with *P. aeruginosa*. As expected, VgrG2b was cleaved in human cells (Fig. 2I). Finally, to verify that *P. aeruginosa* affected inflammasome activation through H2-T6SS, we generated a *P. aeruginosa* strain with VgrG2b deficiency. We found that *P. aeruginosa* lacking VgrG2b no longer inhibited the NLRP3 inflammasome (Fig. 2J and Fig. S2M) and IL-1β could be secreted normally in the mutant bacteria-treated cells (Fig. 2K). However, the percentage of cell death was not affected (Fig. 2L) and the level of cell viability remained unchanged among mutants and wild-type controls (Fig. 2M). These data indicate that H2-T6SS plays an important role in inhibiting

host immune response through VgrG2b during *P. aeruginosa* infection, primarily targeting NLRP3 inflammasome activation rather than caspase-11 activation and GSDMD cleavage.

VgrG2b cleavage at its C-terminus is crucial for NLRP3 inhibition

Caspase-11 recognizes its substrate through a tertiary structure formed by its p22/p10 fragments[40]. To further verify that VgrG2b was a substrate of caspase-11, we co-expressed caspase-11 p22/p10 and VgrG2b in HEK293T cells. Co-immunoprecipitation results showed that VgrG2b bound to the p22/p10 complex (Fig. 3A). VgrG2b also bound to the p22/p10 complex of human caspase-4 (Fig. S3A). These results suggest that VgrG2b can indeed be recognized by caspase-11/4. Based on the size of the cleaved VgrG2b fragment, we speculated that the cleavage site should be at its C-terminus. We constructed mutant plasmids carrying aspartic acid substitutions for VgrG2b and found that only the D883A mutant was no longer cleaved by caspase-11 (Fig. 3B). We also verified that this VgrG2b mutant could not be cleaved by human caspase-4 (Fig. 3C). Meanwhile, we constructed a chimeric protein containing VgrG2a N-terminus, a linker sequence around D883 and VgrG2b C-terminus (Fig. S3B). This chimeric protein could be cleaved by caspase-11 (Fig. 3D). Another chimeric protein containing VgrG2b N-terminus, a linker sequence around D883 and GFP cannot be cleaved by caspase-11 (Fig. S3C). Based on the substrate cleavage characteristic of caspase-11 that it needs to bind the target first to mediate cleavage[40], we speculated that the VgrG2b C-terminus was the site where VgrG2b bound to caspase-11. Therefore, we tested the binding of VgrG2b C-terminus with caspase-11. Indeed, the C-terminus of VgrG2b bound to the p22/p10 complex (Fig. 3E). Similarly, VgrG2b C-terminus also bound to p22/p10 of human caspase-4 (Fig. S3D). VgrG2b was recombinantly expressed and incubated with the p22/p10 complex. We found that caspase-11 induced the cleavage of the recombinant VgrG2b (Fig. 3F).

We generated a *P. aeruginosa* strain with a D883A mutation in the VgrG2b gene. After incubating this bacterium with mouse BMDM, mutant VgrG2b did not undergo cleavage (Fig. 3G). Consistently, the NLRP3 inflammasome was no longer inhibited (Fig. 3H, I) and the secretion of IL-1β was restored post incubation with this *P. aeruginosa*

mutant (Fig. 3J), indicating that VgrG2b cleavage by caspase-11 is crucial for NLRP3 inhibition. The cell death and survival rates were not affected (Fig. 3K, L). Similarly, after incubation of the *P. aeruginosa* mutant with human macrophages, the NLRP3 inflammasome was not suppressed (Fig. S3E, F) and IL-1β was secreted normally (Fig. S3G). The cell death and survival rates were not affected (Fig. S3H, I). These results indicate that VgrG2b cleavage at its C-terminus is crucial for NLRP3 inhibition.

VgrG2b C-terminus interacts with NLRP3

In order to investigate how VgrG2b C-terminus inhibited the NLRP3 inflammasome, we performed a yeast two-hybrid screening using the C-terminus of VgrG2b as a bait and screened a mouse bone marrow cDNA library. In the positive clones obtained from the screening, the NLRP3 fragments repeatedly appeared (Fig. 4A). We validated their interaction in HEK293T cells and found that VgrG2b C-terminus indeed bound to NLRP3 (Fig. 4B). Full-length VgrG2b also bound to NLRP3 (Fig. 4C), but the N-terminus of VgrG2b did not bind to NLRP3 (Fig. S4A). VgrG2b C-terminus was introduced into BMDM cells through cell-penetrating peptides, and it was found that the C-terminus interacted with endogenous NLRP3 (Fig. 4D). Similarly, VgrG2b C-terminus also interacted with the human NLRP3 (Fig. S4B). In addition, we incubated *P. aeruginosa* with mouse BMDM cells and found that NLRP3 interacted with the C-terminus of VgrG2b rather than the full-length one (Fig. 4E). The same result was observed after incubation of *P. aeruginosa* with human macrophages, where NLRP3 bound to the C-terminus of VgrG2b (Fig. S4C). The colocalization between VgrG2b C-terminus and NLRP3 was observed inside BMDM cells (Fig. 4F). The VgrG2b C-terminus did not bind to mouse GSDMD (Fig. S4D), ASC (Fig. S4E), nor caspase-1 (Fig. S4F), indicating that the binding targets of VgrG2b in host cells is very specific. We further searched for the region where VgrG2b C-terminus interacted with NLRP3 (Fig. 4G), and found that their interaction area was at the NACHT-LRR junction of NLRP3 (Fig. 4H, I).

In *Casp11* knockout BMDM cells, VgrG2b could not be cleaved and did not bind to NLRP3 (Fig. 4J). However, in *Gsdmd* knockout cells, VgrG2b still underwent cleavage and bound to NLRP3 (Fig. S4G). In the absence of GSDMD, the NLRP3 inflammasome was not activated[5,37]. This result indicates that the binding of VgrG2b C-terminus to

NLRP3 is independent of NLRP3 activation, but requires a cleaved segment of VgrG2b processed by caspase-11. In all, these results suggest that the cleaved VgrG2b C-terminus binds NLRP3.

VgrG2b C-terminus suppresses the NLRP3 inflammasome

Whether VgrG2b C-terminus directly inhibited the activation of NLRP3 inflammasomes was the focus of our next exploration. We validated this hypothesis in the HEK293T recombination system. The VgrG2b C-terminus significantly inhibited the activation of NLRP3 inflammasome originated from mouse (Fig. 5A) or human (Fig. S5A). In addition, overexpression of VgrG2b C-terminus suppressed the activation of classical NLRP3 inflammasomes in both mouse (Fig. 5B) and human macrophages (Fig. S5B). These data indicate that VgrG2b C-terminus exhibits a broad-spectrum inhibition of the NLRP3 inflammasome. Introducing VgrG2b C-terminus into BMDM cells through cell-penetrating peptides can significantly inhibit the activation of NLRP3 post intracellular LPS stimulation, without affecting the activation of caspase-11 and GSDMD (Fig. 5C, D). The secretion of IL-1β was significantly decreased (Fig. 5E). The cell death (Fig. 5F) and survival rates (Fig. 5G) were not affected. The activation of NLRP3 could also be inhibited by introducing VgrG2b C-terminus through cell-penetrating peptides when classical NLRP3 inflammasomes stimuli were present (Fig. S5C), accompanied by a reduction of IL-1β secretion (Fig. S5D), a decrease in cell death (Fig. S5E) and an increase in cell viability (Fig. S5F).

We next searched for the specific mechanism by which VgrG2b C-terminus inhibited the NLRP3 inflammasome. We first tested the ability of NLRP3 to catalyze ATP hydrolysis after the addition of VgrG2b C-terminus and found that the hydrolysis potential of NLRP3 was not affected (Fig. S5G). Meanwhile, VgrG2b C-terminus did not influence the binding of NLRP3 to mitochondrial DNA (Fig. S5H), as well as to Nur77 (Fig. 5H). The binding of NLRP3 to NEK7 was immensely inhibited by the C-terminus of VgrG2b (Fig. 5I). VgrG2b C-terminus did not bind to NEK7 (Fig. S5I). Domain mapping showed that the VgrG2b C-terminus bound to the same NLRP3 segment as NEK7 (Fig. 4G–I). We therefore detected the competitive binding between VgrG2b C-terminus and NEK7 to NLRP3. VgrG2b C-terminus competed against NEK7 (Fig. 5J), while NEK7 couldn’t

compete with VgrG2b C-terminus (Fig. S5J), indicating that VgrG2b C-terminus has a stronger binding ability with NLRP3 compared to NEK7.

VgrG2b cleavage is essential for *P. aeruginosa* infection

Finally, we infected mice with a *P. aeruginosa* strain carrying a D883A mutation in the VgrG2b gene. The survival rate of mice was greatly improved when infected with the mutant strain (Fig. 6A). the level of IL-1β in the serum was also increased (Fig. 6B), while other inflammatory cytokines such as TNF-α and IL-6 showed little difference among wild-type and mutant bacteria (Fig. 6C, D). The bacterial load in the lungs of mice infected with the mutant strain was also decreased (Fig. 6E). We also detected the activation of inflammasomes in macrophages from lung lavage fluid and found that the activation of the NLRP3 inflammasome was activated in cells infected with the mutant strain (Fig. 6F), but the cell viability was not affected (Fig. 6G). We detected the protein levels of cytokines in the lavage fluid and found that the level of IL-1β was increased from mice infected with *P. aeruginosa* mutant strain (Fig. 6H). Other inflammatory cytokines such as TNF-α and IL-6 showed little difference (Fig. 6I, J).

We designed a short peptide of VgrG2b C-terminus containing the VgrG2b linker region with a D883A substitution and a transmembrane TAT sequence. Peptides were then myristoylated[41], aiming to target this peptide to inner membrane and suppress bacterial VgrG2b cleavage through competing with wild-type VgrG2b for caspase-11 (Fig. S6A). We first conducted tests at the cellular level and found that adding this peptide to BMDM cells after incubation with *P. aeruginosa* relieved the inhibition of the NLRP3 inflammasome (Fig. S6B) and the secretion of IL-1β was significantly increased (Fig. S6C). The cell death rate did not change significantly and the viability rate was not affected by this peptide (Fig. S6D, E). The same effect was observed in human macrophages, where this designed peptide could relieve the inhibition of *P. aeruginosa* on the NLRP3 inflammasome (Fig. S6F) and the secretion of cytokine IL-1β was also increased (Fig. S6G). Although it had no effect on cell death and viability (Fig. S6H, I), Finally, we delivered this peptide into the lungs of mice infected with *P. aeruginosa* through nebulization, and found that the survival rate of mice was increased (Fig. 6K). The level of IL-1β in the serum was increased (Fig. 6L), while other inflammatory factors such

as TNF-α and IL-6 remained unchanged (Fig. 6M, N). The bacterial load was also decreased (Fig. 6O), indicating the potential medicinal value of this designed peptide in the future clinical treatment of *P. aeruginosa* infections.

Discussion

In this study, we found that the structural protein VgrG2b from *P. aeruginosa* can be cleaved by caspase-11 in host cells. The C-terminal fragment of VgrG2b bound to NLRP3, inhibiting the activation of the NLRP3 inflammatory and the secretion of IL-1β. The delivery of VgrC2b C-terminus mimics significantly improved the infection symptoms caused by *P. aeruginosa*, providing an optional treatment approach for chronic infections of *P. aeruginosa*.

The infection of *P. aeruginosa*, especially those in chronic infections, is an important factor causing pulmonary fibrosis in clinicals[13,17]. LPS from Gram-negative bacterium can be transported to host cells and activate non-canonical inflammasomes within them[2,3]. There are many ways for LPS from bacteria to be transported into host cells, including binding with HMGB1 originated from the liver and entering the interior of the cells through the surface of macrophages, as well as enveloping and delivering LPS into the host cells through extracellular vesicles[42,43]. We observed the activation of non-canonical inflammasomes in macrophages after infection with *P. aeruginosa*, indicating that LPS was also transported into the cells. *P. aeruginosa* is not a typical intracellular bacterium, and its LPS entry into target cells is likely through the out membrane vesicles *in vivo*.

P. aeruginosa mainly utilizes the T6SS secretion system to promote the establishment of chronic infections[17]. During this process, H2-T6SS plays many important roles, responsible for delivering known and yet to be explored virulence factors into host cells[23,28]. Here we have found that VgrG2b is not only responsible for the delivery of bacterial virulence proteins, but it can also serve as a virulence factor on its own. Its uniqueness lies in the fact that it requires cutting to be effective. Whether there are other proteins secreted through the H2-T6SS in *P. aeruginosa* that need to be cleaved by host proteases before they exert their function is a very worthwhile research topic. Of course, this processing from the host is not limited to cleavage, but may also be post-translational modifications of proteins such as phosphorylation or ubiquitination[44,45]. Systematically

identifying these possible modifications and their substrates will be of great significance for understanding the pathogenic mechanism of *P. aeruginosa*.

The non-canonical inflammasome receptor caspase-11 has a very narrow substrate spectrum[39]. The process of substrate cleavage by inflammatory caspases can be divided into two parts. Firstly, inflammatory caspases bind to a part of the substrate, which is often not their cleavage site, and the other is the recognition of the true site of their cleavage. This mechanism ensures that limited proteins are cleaved by host cells when inflammasomes are activated, thereby confining the severity of the inflammatory response. Here, we found that caspase-11/4 specifically cleaves the structural proteins of the secretion system of *P. aeruginosa*, and the generated new fragments can play an inhibitory role. This is a new way for pathogenic microorganisms to hijack the host's immune system. Because traditional hijacking usually directly affects the host immune system without cutting. It is very effective for *P. aeruginosa* using VgrG2b fragment to inhibit NLRP3. On the one hand, VgrG2b transports virulence factors into the host cell, and on the other hand, the cleaved substrate plays a role in inhibiting the NLRP3 inflammasome.

In summary, we have discovered a new pattern of recognition between bacterial proteins and the host immune system during *P. aeruginosa* infection, which involves hijacking the host's protease to produce a new virulence factor that can inhibit the host's immune response.

Experimental procedures

Antibodies and reagents

Antibodies against NLRP3 (15101), IL-1β (12703, 12426), cleaved IL-1β (83186, 63124), GSDMD (93709), caspase-1 (3866, 24232, 2225) and ASC (13833, 67824) were purchased from Cell Signaling Technology. Antibodies against caspase-1 (ab207802) and GSDMD (ab215203) were purchased from Abcam. Antibodies against caspase-11 were: ab180673 from Abcam, 14340 from Cell Signaling Technology, 14-9935-82 from Invitrogen, M029-3 from MBL Beijing Biotech. Anti-c-Myc magnetic beads (88843) were purchased from Pierce. Antibody against 6xHis tag (MA121315) was purchased from

Invitrogen. Antibodies against FLAG tag (F3165), β-actin (A1978) and anti-FLAG M2 magnetic beads (M8823) were purchased from Sigma-Aldrich. Antibodies against c-Myc (sc-40) and GST (sc-138) were purchased from Santa Cruz Biotechnology. Anti-HA tag antibody (HX1820) was purchased from Huaxingbio (Beijing). HRP-conjugated goat anti-mouse IgG (SA00001-1) and HRP-conjugated goat anti-rabbit IgG (SA00001-2) were purchased from Proteintech Group. Alexa Fluor Plus 488-conjugated goat anti-mouse IgG (A32723) and Alexa Fluor 594-conjugated goat anti-rabbit IgG (A32740) were purchased from Invitrogen. Alexa Fluor Plus 488-conjugated donkey anti-goat IgG (bs-0294D-AF488) and Alexa Fluor 594-conjugated donkey anti-rabbit IgG (bs-0295D-AF594) were purchased from Bioss (Beijing).

Glutathione sepharose 4B resin (17075601) was purchased from Cytiva. Protein A/G PLUS-Agarose beads (sc-2003) were purchased from Santa Cruz Biotechnology. DAPI (2879038) was purchased from PeproTech (BioGems). SMART MMLV reverse transcriptase (639524) was purchased from Clontech, Takara Bio. Random primer (Hexadeoxyribonucleotide mixture, pd(N)6) (3801) was purchased from Takara Bio. Protease inhibitor cocktail (11697498001) was purchased from Roche. Total RNA extraction kit (8034111) was purchased from Dakewe (Beijing). Ni-NTA agarose beads (R90115) and AminoLink coupling resin (20381) were purchased from Invitrogen. LPS (B46894) was purchased from Innochem (Beijing). DOTAP was: D10530 from Psaitong (Beijing) and 11202375001 from Roche. Nigericin (481990), Gramicidin (368020), ATP (A6559) were purchased from Merck Millipore. Cell-penetrating peptides: ab142343 from Abcam and sc-396807 from Santa Cruz. Human M-CSF (300-25) and murine M-CSF (315-02) were purchased from PeproTech. CellTiter-Glo luminescent cell viability assay kit (G7570) and CytoTox 96 non-radioactive cytotoxicity assay kit (G1780) were purchased from Promega.

Bacteria and CFU determination

E. coli (CGMCC1.2389, ATCC11775) was from China General Microbiological Culture Collection Center. *Pseudomonas aeruginosa* (PAO1) was a gift from Dr. Lvyan Ma (Institute of Microbiology, Chinese Academy of Sciences). *E. coli* and *P. aeruginosa* were preserved in LB plates and inoculated to liquid LB medium, followed by shaking at 37 °C

until they grew to the exponential phase (optical density=0.6–0.8). Bacteria were diluted and spread into LB plates to determine the CFU numbers. When the bacteria were cultured to the mid-exponential stage, they were washed three times with PBS and resuspended in PBS or DMEM.

***P. aeruginosa* OMV purification**

When *P. aeruginosa* was cultured to the mid exponential stage, cultures were centrifugated to obtain the supernatant. After filtering through a 0.22 μm filter, the supernatant was placed in a discontinuous sucrose gradient tube and centrifuged at a speed of 100, 000 g for 16 h. The precipitate was resuspended by PBS and centrifuged again to remove residual culture medium components. The precipitate was resuspended with PBS again, resulting in the OMV sample. The sample was immediately used or frozen and stored in a –80 °C freezer. 20 μg/ml OMV was used in each *in vitro* experiment.

***P. aeruginosa* knockout and knockin strategy**

The knockout plasmid pK18mobsacBGm was digested with BamHI and HindIII, and then recovered by agarose gel electrophoresis. Primers were designed to clone homologous arms of approximately 900 bp upstream and downstream of the target gene. This knockout strategy preserved the starting 99bp and ending 99bp of the target gene. The upstream and downstream homologous arms were then connected with the linearized pk18mobsacBGm vector using homologous recombination, and the knockout vector pk18mobsacBGm-target were obtained through sequencing. Primers used were: RetS-up-F: 5’-ctcggtacccggggatccccgccgtgcgcgacatgctcgccggcaa-3’, RetS-up-R: 5’-agcacgtcgctgc ccggcgaagtcccttcg-3’, RetS-down-F: 5’-ccttcgaagggacttcgccgggcagcgacgtgctccgg-3’, RetS-down-R: 5’-cgttgtaaaacgacggccagtgccaagcttcgagggtcaggcaggcgag-3’ for RetS knockout; KO-VgrG2b-up-F: 5’-attcgagctcggtacccggggatcccttgatggaaaagagtttcaagacc-3’, KO-VgrG2b-up-R: 5’-tctcgaggaaataatctcgaacgataggctcgcagagcgcttcttccagt-3’, KO-VgrG2b-down-F: 5’-actggaagaagcgctctgcgagcctatcgttcgagattatttcctcga-3’, KO-VgrG2b-down-R: 5’-taaaacgacggccagtgccaagcttgacgacgtcggggttctctgcctt-3’ for VgrG2b knockout; KI-Myc-VgrG2b-up-F:

5’-tcgagctcggtacccggggatccgagcacatcaccctgatgtgcggcggcgcct-3’, KI-Myc-VgrG2b-up-R1: 5’-ttcgaaccgcgggccctctagactcgagcggtatcccgttgggaagtttttcagt-3’, KI-Myc-VgrG2b-up-R2: 5’-atcctcttctgagatgagtttttgttcgaaccgcgggccctctagactc-3’, KI-Myc-VgrG2b-down-F: 5’-aaaaactcatctcagaagaggatctgtgaccaatgaaatgcaagaccttgctca-3’, KI-Myc-VgrG2b-down-R: 5’-taaaacgacggccagtgccaagcttcggccccgccggcgccactggcgaa-3’ for VgrG2b-Myc knockin; VgrG2b-D883A-up-F: 5’-aattcgagctcggtacccggggatccgagcaccagg gcgtggggcacgacg-3’, VgrG2b-D883A-up-R: 5’-aggtcttgcatttcattggtcacagatcctcttctgagat gag-3’, VgrG2b-D883A-down-F: 5’-actcatctcagaagaggatctgtgaccaatgaaatgcaagaccttgctc a-3’, VgrG2b-D883A-down-R: 5’-taaaacgacggccagtgccaagcttttcgccggccaggcagaattcgacg-3’ for VgrG2b D883A knockin. The recipient bacterium *P. aeruginosa*, co-plasmid pRK2013, and donor bacterium (pK18mobsacBGm-target) were inoculated in LB liquid medium (with corresponding antibiotics added), and incubated overnight in a shaking table at 37 °C and 200 rpm. 1 ml of co-plasmid and donor bacterial culture medium were collected separately and centrifuged at 5, 000 rpm for 2 m. Pellets were collected and resuspended in 200 μl LB medium. Co-plasmids and donor bacteria were mixed in a 1:1 ratio, and inoculated on LB solid culture medium at 37 °C for 2 hours. Simultaneously, the recipient strain *P. aeruginosa* was placed in 42 °C for 2 hours of cultivation. 1mL of receptor bacteria was collected and centrifuged at 5, 000 rpm for 2 min and resuspended in 200 μl LB liquid medium. The bacteria were spotted onto a mixed plaque of co-plasmids and donor bacteria and cultured at 37 °C for 4 hours. The plaque was picked up and suspended in the 500–800 μl LB liquid medium and plated onto LB plates with Irg and Gm resistance, followed by culture overnight at 37 °C. A single colony was selected and transferred again to LB plates with Irg and Gm resistance. The next day, bacteria were drawn a line on a 20–22% sucrose agar plate and cultured at 37 °C for 24–48 hours. Single colonies were selected again according to the above method. Colonies that could grow on LB plates but not on Gm resistant plates were chosen and subjected to PCR validation.

Cell component fractionation and mitochondrial DNA quantification

Cells were fractionated according to the guidelines of a cell fractionation kit from Abcam (ab109719). Mitochondria were isolated from macrophages using a mitochondrial

isolation kit from Abcam (ab110170) or from Invitrogen (89874), followed by mitochondrial DNA purification through a mitochondrial DNA isolation kit from Abcam (ab65321). Total cytosolic DNA was extracted using a DNeasy Blood & Tissue Kit (QIAGEN) following manufacturer's instructions. For mitochondrial DNA quantification, samples containing mitochondrial DNA were subjected to RT-PCR analyses using the following primers: 5'-GAGATGACCAAATTTACAATG-3' (forward) and 5'-TCCTGTTCCTGCTCCTGCTTC-3' (reverse) for mouse mitochondrial gene COX1.

Mice and infection

Casp4$^{-/-}$ (S-KO-01332), *Gsdmd*$^{-/-}$ (S-KO-12963) and *Aim2*$^{-/-}$ (S-KO-09889) mice were purchased from Cyagen Biosciences (Jiangsu, China). Mice were intraperitoneally challenged with poly(I:C) at a dose of 2 mg/kg body weight for 6 h and then intranasally infected with $1x10^9$ cfu of *P. aeruginosa* strain PAO1, followed by survival calculation at the indicated days. Sera were collected and subjected to ELISA assays. For bronchoalveolar lavage fluid (BALF) collection, mice were anaesthetized, followed by thoracic cavity opened and a flush of circulating blood cells by injecting about 10 ml ice-cold PBS into the right ventricle. Mouse neck was then dissected to expose trachea. A puncture needle was inserted into the upper end of the trachea, followed by repeated rinsing with 0.8 ml PBS for five times. BALF collections were centrifuged at 300 g at 4 °C for 5 min, followed by ELISA assays of the supernatants or macrophage isolation in the cell pellets.

Primary cell separation and culture

To generate BMDM cells, bone marrow cells were flushed from mouse femurs and tibias, followed by red blood cell removal using red blood cell lysis buffer. Cells were resuspended in alpha-MEM containing 10% (v/v) fetal bovine serum and 10 ng/ml M-CSF and grown at 37 °C with a 5% CO_2 humidified atmosphere for 7 days. To produce human macrophages, human bloods collected from healthy donors were mixed with an equal volume of saline and then added to lymphocyte separation medium, followed by centrifugation and PBMC collection. Human PBMCs were incubated with APC-conjugated anti-CD14 antibody on ice for 30 min, followed by incubation with anti-APC-conjugated magnetic beads. Monocytes were enriched on a magnetic separator. To test the purity of

sorted monocytes, cells were stained with APC conjugated anti-CD14 antibody, followed by FACS examination. Cells with purity above 95% were used for subsequent experiments. Cells were resuspended in RPMI-1640 medium containing 10% (v/v) fetal bovine serum and 50 ng/ml human M-CSF, followed by growing at 37 °C with a 5% CO_2 humidified atmosphere for 7 days. Healthy blood samples were provided by the researchers volunteering. Informed consents were obtained from all subjects and experiments conformed to related principles. Study was licensed by the Ethics Committee of Institute of Microbiology, Chinese Academy of Sciences.

Inflammasome induction

For canonical NLRP3 inflammasome activation, cells were incubated with 1 μg/ml LPS for 3 h, followed by stimulation with 10 μM nigericin for 30 min, 0.5 μM gramicidin for 1 h and 2 mM ATP for 30 min. Cells were grown at 37 °C with a 5% CO_2 humidified atmosphere. For non-canonical inflammasome stimulation, macrophages were primed overnight with 1 μg/ml Pam3CSK4, followed by transfection of 2 μg/ml LPS using DOTAP for 16 h. Otherwise, macrophages were primed overnight with 1 μg/ml Pam3CSK4 and incubated with *P. aeruginosa* strain PAO1 at an MOI of 30 and OMVs for 2 h. Cells were then supplemented with fresh medium containing 100 μg/ml Gentamycin and cultured for 16 h.

Plasmid transfection and lentiviral production

Transfection reagent JetPRIME (Polyplus Transfection) was used to conduct transfection in HEK293T cells. HEK293T cells were plated 14 h earlier to achieve a density of about 70% when transfection was performed. Lentiviral plasmids containing exogenous genes of interest and packaging plasmids pSPAX2 and pMD2.G were transfected into HEK293T cells at a ratio of 4:3:1. 48 h later, supernatants were collected, followed by centrifugation at 1,000 rpm for 5 min and filtration using 0.45 μm sterile syringe filters (Merck Millipore). The filtrate was then concentrated with a 100 kD Amicon ultra centrifugal filter unit (Merck Millipore). Macrophage cells were incubated with lentiviruses for 6 h, followed by culture medium replacement with fresh medium. 2 μg/ml puromycin was added to the medium 48 h post infection for 3 days.

Cell viability and cytotoxicity assay

Cell pellets from cells stimulated with inflammasome activators were used to measure cell viability through checking cellular ATP levels with a CellTiter-Glo luminescent cell viability assay kit (Promega). The supernatants from cells stimulated with inflammasome activators were collected and subjected to lactate dehydrogenase (LDH) assay to assess cell death using a CytoTox 96 non-radioactive cytotoxicity assay kit (Promega). Both the supernatants and cell pellets were collected for immunoblotting analyses.

ELISA

ELISA kits detecting human IL-1β (D711068), mouse IL-1β (D721017), mouse IL-6 (D721022) and mouse TNF-α (D721217) were purchased from BBI life sciences (Shanghai). Cell culture supernatants were collected and subjected to ELISA assays following manufacturer's instructions.

Recombinant protein expression and purification

For recombinant expression of GST-tagged proteins, cDNA of interest was cloned into pGEX-6P-1 vector. Plasmids were transformed into *E. coli* strain BL21 and the bacteria grew in LB medium supplemented with 100 μg/ml ampicillin at 37 °C for 8 h, followed by addition of IPTG to a final concentration of 0.5 mM and shaking at 150 rpm at 37 °C for 3 h. Cells were harvested and resuspended with PBS containing 1% Triton-X-100 and lysed by sonication. Cell lysates were centrifuged at 13,000 rpm at 4 °C for 30 min and filtered through sterile syringe filters. For crude purification of recombinant proteins, the filtered lysate was loaded on column containing glutathione sepharose 4B resin, followed by washing with PBS containing 1% Triton-X-100. The protein was eventually eluted by 1 ml 10 mM L-Glutathione solution. For removal of LPS contaminations, crudely purified proteins were further eluted through Pierce high-capacity endotoxin removal spin columns and heparin columns to remove LPS and bacterial genomic DNA, respectively. GST tags were removed by a PreScission protease.

Immunoprecipitation

HEK293T cells were seeded on 6-well culture plates and were transfected with plasmids 16 h later. 24 h post transfection, cells were washed twice with PBS and lysed in a pre-chilled buffer containing 150 mM NaCl, 50 mM Tris (pH 7.5), 1 mM EDTA, 0.5%

digitonin, 1% protease inhibitor cocktail and 10% glycerol on ice for 30 min. For immunoprecipitation using primary cells, cells post stimulation or treatments were lysed in a pre-chilled PBS buffer containing 0.5% digitonin, 1% protease inhibitor cocktail on ice for 30 min. Cell lysates were centrifuged at 13,000 rpm at 4 °C for 10 min. Primary antibodies and their isotype control IgG were immobilized to AminoLink Coupling Resin (ThermoFisher Scientific) following the manufacturer's instructions. Supernatants were incubated with immobilized antibodies at 4 °C for 2 h. Resins were washed three times with PBS containing 0.5% digitonin, followed by immunoprecipitant detachment in 0.1 M Glycine-HCl, pH 2.7. Supernatants were neutralized by adding 1/10 the volume of 2 M Tris-HCl, pH 8.0, followed by immunoblotting with the indicated antibodies.

Immunofluorescence

Cells adhered to covers pre-coated with poly-L-lysine were stimulated with inflammasome activators, followed by fixation with 4% paraformaldehyde for 10 min at room temperature. Cells were then washed twice with PBS and permeabilized with PBS containing 0.1% digitonin for 10 min, followed by washing with PBS for twice and blockage in 10% normal goat serum at 37 °C for 30 min. Cells were incubated with primary antibody for 2 h, followed by washing with PBS for three times and further incubation with fluorescence-conjugated secondary antibody for 1 h. Nuclei were stained with DAPI. Cells were visualized through an UltraVIEW VoX imaging system (PerkinElmer).

Statistical analysis

No statistical methods were used to predetermine sample size. Experiments were independently repeated at least three times to achieve statistical significance. No randomization or blinding procedures was used in this study. No samples were excluded from the analysis. Data were shown as means ± SD of three technical replicates. Data with normal distribution determined by Shapiro–Wilk normality test were statistically analyzed by two tailed Student's t tests if not specified. The Gehan-Breslow-Wilcoxon test was used for the analysis of survival data. Data were analyzed by GraphPad Prism 9.0. P-values ≤ 0.05 were termed as significant; NS means non-significant where $P > 0.05$.

Acknowledgements

We thank Yingyu Chen (Peking University) for technical help. This work was supported by the National Natural Science Foundation of China (92369104, 82271790, 92169113), Beijing Natural Science Foundation (JQ23028, 7212067), the National Key R&D Program of China (2021YFA1300202, 2022YFC2302900), Strategic Priority Research Programs of the Chinese Academy of Sciences (XDB29020000), Key Research Program of Frontier Sciences of Chinese Academy of Sciences (ZDBS-LY-SM025), CAS Project for Young Scientists in Basic Research (YSBR-010), Fok Ying Tung Education Foundation to P.X., Youth Innovation Promotion Association of CAS to S.W.

Author contributions

Y.Q. and Q.L. performed experiments and analyzed data; W.L., C.W., C.K., M.L. and S.W. performed experiments; P.X. initiated the study, designed and performed experiments, analyzed data, and wrote the paper.

References

1. Hagar, J.A., Powell, D.A., Aachoui, Y., Ernst, R.K., and Miao, E.A. (2013). Cytoplasmic LPS activates caspase-11: implications in TLR4-independent endotoxic shock. Science (New York, N.Y.) *341*, 1250-1253. 10.1126/science.1240988.
2. Kayagaki, N., Wong, M.T., Stowe, I.B., Ramani, S.R., Gonzalez, L.C., Akashi-Takamura, S., Miyake, K., Zhang, J., Lee, W.P., Muszyński, A., et al. (2013). Noncanonical inflammasome activation by intracellular LPS independent of TLR4. Science (New York, N.Y.) *341*, 1246-1249. 10.1126/science.1240248.
3. Shi, J., Zhao, Y., Wang, Y., Gao, W., Ding, J., Li, P., Hu, L., and Shao, F. (2014). Inflammatory caspases are innate immune receptors for intracellular LPS. Nature *514*, 187-192. 10.1038/nature13683.
4. Huang, L.S., Hong, Z., Wu, W., Xiong, S., Zhong, M., Gao, X., Rehman, J., and Malik, A.B. (2020). mtDNA Activates cGAS Signaling and Suppresses the YAP-Mediated Endothelial Cell Proliferation Program to Promote Inflammatory Injury. Immunity *52*, 475-486.e475. 10.1016/j.immuni.2020.02.002.
5. Kayagaki, N., Stowe, I.B., Lee, B.L., O'Rourke, K., Anderson, K., Warming, S., Cuellar, T., Haley, B., Roose-Girma, M., Phung, Q.T., et al. (2015). Caspase-11 cleaves gasdermin D for non-canonical inflammasome signalling. Nature *526*, 666-671. 10.1038/nature15541.
6. Shi, J., Zhao, Y., Wang, K., Shi, X., Wang, Y., Huang, H., Zhuang, Y., Cai, T., Wang, F., and Shao, F. (2015). Cleavage of GSDMD by inflammatory caspases determines

pyroptotic cell death. Nature *526*, 660-665. 10.1038/nature15514.

7. Rathinam, V.A.K., Zhao, Y., and Shao, F. (2019). Innate immunity to intracellular LPS. Nature immunology *20*, 527-533. 10.1038/s41590-019-0368-3.
8. Barnett, K.C., Li, S., Liang, K., and Ting, J.P. (2023). A 360° view of the inflammasome: Mechanisms of activation, cell death, and diseases. Cell *186*, 2288-2312. 10.1016/j.cell.2023.04.025.
9. Christgen, S., Place, D.E., and Kanneganti, T.D. (2020). Toward targeting inflammasomes: insights into their regulation and activation. Cell research *30*, 315-327. 10.1038/s41422-020-0295-8.
10. He, Y., Zeng, M.Y., Yang, D., Motro, B., and Núñez, G. (2016). NEK7 is an essential mediator of NLRP3 activation downstream of potassium efflux. Nature *530*, 354-357. 10.1038/nature16959.
11. Zhu, F., Ma, J., Li, W., Liu, Q., Qin, X., Qian, Y., Wang, C., Zhang, Y., Li, Y., Jiang, D., et al. (2023). The orphan receptor Nur77 binds cytoplasmic LPS to activate the non-canonical NLRP3 inflammasome. Immunity *56*, 753-767.e758. 10.1016/j.immuni.2023.03.003.
12. Cendra, M.D.M., and Torrents, E. (2021). Pseudomonas aeruginosa biofilms and their partners in crime. Biotechnology advances *49*, 107734. 10.1016/j.biotechadv.2021.107734.
13. Rossi, E., La Rosa, R., Bartell, J.A., Marvig, R.L., Haagensen, J.A.J., Sommer, L.M., Molin, S., and Johansen, H.K. (2021). Pseudomonas aeruginosa adaptation and evolution in patients with cystic fibrosis. Nature reviews. Microbiology *19*, 331-342. 10.1038/s41579-020-00477-5.
14. Goodman, A.L., Kulasekara, B., Rietsch, A., Boyd, D., Smith, R.S., and Lory, S. (2004). A signaling network reciprocally regulates genes associated with acute infection and chronic persistence in Pseudomonas aeruginosa. Dev Cell *7*, 745-754. 10.1016/j.devcel.2004.08.020.
15. Faure, E., Mear, J.B., Faure, K., Normand, S., Couturier-Maillard, A., Grandjean, T., Balloy, V., Ryffel, B., Dessein, R., Chignard, M., et al. (2014). Pseudomonas aeruginosa type-3 secretion system dampens host defense by exploiting the NLRC4-coupled inflammasome. American journal of respiratory and critical care medicine *189*, 799-811. 10.1164/rccm.201307-1358OC.
16. Hauser, A.R. (2009). The type III secretion system of Pseudomonas aeruginosa: infection by injection. Nature reviews. Microbiology *7*, 654-665. 10.1038/nrmicro2199.
17. Qin, S., Xiao, W., Zhou, C., Pu, Q., Deng, X., Lan, L., Liang, H., Song, X., and Wu, M. (2022). Pseudomonas aeruginosa: pathogenesis, virulence factors, antibiotic resistance, interaction with host, technology advances and emerging therapeutics. Signal transduction and targeted therapy *7*, 199. 10.1038/s41392-022-01056-1.
18. Hachani, A., Lossi, N.S., Hamilton, A., Jones, C., Bleves, S., Albesa-Jové, D., and Filloux, A. (2011). Type VI secretion system in Pseudomonas aeruginosa: secretion and multimerization of VgrG proteins. The Journal of biological chemistry *286*, 12317-12327. 10.1074/jbc.M110.193045.
19. Mougous, J.D., Cuff, M.E., Raunser, S., Shen, A., Zhou, M., Gifford, C.A., Goodman, A.L., Joachimiak, G., Ordoñez, C.L., Lory, S., et al. (2006). A virulence locus of Pseudomonas aeruginosa encodes a protein secretion apparatus. Science (New York, N.Y.) *312*,

1526-1530. 10.1126/science.1128393.
20. Chen, L., Zou, Y., She, P., and Wu, Y. (2015). Composition, function, and regulation of T6SS in Pseudomonas aeruginosa. Microbiological research *172*, 19-25. 10.1016/j.micres.2015.01.004.
21. Ho, B.T., Dong, T.G., and Mekalanos, J.J. (2014). A view to a kill: the bacterial type VI secretion system. Cell host & microbe *15*, 9-21. 10.1016/j.chom.2013.11.008.
22. Hood, R.D., Singh, P., Hsu, F., Güvener, T., Carl, M.A., Trinidad, R.R., Silverman, J.M., Ohlson, B.B., Hicks, K.G., Plemel, R.L., et al. (2010). A type VI secretion system of Pseudomonas aeruginosa targets a toxin to bacteria. Cell host & microbe *7*, 25-37. 10.1016/j.chom.2009.12.007.
23. Jiang, F., Waterfield, N.R., Yang, J., Yang, G., and Jin, Q. (2014). A Pseudomonas aeruginosa type VI secretion phospholipase D effector targets both prokaryotic and eukaryotic cells. Cell host & microbe *15*, 600-610. 10.1016/j.chom.2014.04.010.
24. Russell, A.B., LeRoux, M., Hathazi, K., Agnello, D.M., Ishikawa, T., Wiggins, P.A., Wai, S.N., and Mougous, J.D. (2013). Diverse type VI secretion phospholipases are functionally plastic antibacterial effectors. Nature *496*, 508-512. 10.1038/nature12074.
25. Durand, E., Cambillau, C., Cascales, E., and Journet, L. (2014). VgrG, Tae, Tle, and beyond: the versatile arsenal of Type VI secretion effectors. Trends in microbiology *22*, 498-507. 10.1016/j.tim.2014.06.004.
26. Leiman, P.G., Basler, M., Ramagopal, U.A., Bonanno, J.B., Sauder, J.M., Pukatzki, S., Burley, S.K., Almo, S.C., and Mekalanos, J.J. (2009). Type VI secretion apparatus and phage tail-associated protein complexes share a common evolutionary origin. Proceedings of the National Academy of Sciences of the United States of America *106*, 4154-4159. 10.1073/pnas.0813360106.
27. Shneider, M.M., Buth, S.A., Ho, B.T., Basler, M., Mekalanos, J.J., and Leiman, P.G. (2013). PAAR-repeat proteins sharpen and diversify the type VI secretion system spike. Nature *500*, 350-353. 10.1038/nature12453.
28. Sana, T.G., Baumann, C., Merdes, A., Soscia, C., Rattei, T., Hachani, A., Jones, C., Bennett, K.L., Filloux, A., Superti-Furga, G., et al. (2015). Internalization of Pseudomonas aeruginosa Strain PAO1 into Epithelial Cells Is Promoted by Interaction of a T6SS Effector with the Microtubule Network. mBio *6*, e00712. 10.1128/mBio.00712-15.
29. Wood, T.E., Howard, S.A., Förster, A., Nolan, L.M., Manoli, E., Bullen, N.P., Yau, H.C.L., Hachani, A., Hayward, R.D., Whitney, J.C., et al. (2019). The Pseudomonas aeruginosa T6SS Delivers a Periplasmic Toxin that Disrupts Bacterial Cell Morphology. Cell reports *29*, 187-201.e187. 10.1016/j.celrep.2019.08.094.
30. Balakrishnan, A., Karki, R., Berwin, B., Yamamoto, M., and Kanneganti, T.D. (2018). Guanylate binding proteins facilitate caspase-11-dependent pyroptosis in response to type 3 secretion system-negative Pseudomonas aeruginosa. Cell Death Discov *4*, 3. 10.1038/s41420-018-0068-z.
31. Huus, K.E., Joseph, J., Zhang, L., Wong, A., Aaron, S.D., Mah, T.F., and Sad, S. (2016). Clinical Isolates of Pseudomonas aeruginosa from Chronically Infected Cystic Fibrosis Patients Fail To Activate the Inflammasome during Both Stable Infection and Pulmonary Exacerbation. J Immunol *196*, 3097-3108. 10.4049/jimmunol.1501642.
32. Phuong, M.S., Hernandez, R.E., Wolter, D.J., Hoffman, L.R., and Sad, S. (2021).

Impairment in inflammasome signaling by the chronic Pseudomonas aeruginosa isolates from cystic fibrosis patients results in an increase in inflammatory response. Cell death & disease *12*, 241. 10.1038/s41419-021-03526-w.

33. Allsopp, L.P., Wood, T.E., Howard, S.A., Maggiorelli, F., Nolan, L.M., Wettstadt, S., and Filloux, A. (2017). RsmA and AmrZ orchestrate the assembly of all three type VI secretion systems in Pseudomonas aeruginosa. Proceedings of the National Academy of Sciences of the United States of America *114*, 7707-7712. 10.1073/pnas.1700286114.
34. Han, Y., Wang, T., Chen, G., Pu, Q., Liu, Q., Zhang, Y., Xu, L., Wu, M., and Liang, H. (2019). A Pseudomonas aeruginosa type VI secretion system regulated by CueR facilitates copper acquisition. PLoS pathogens *15*, e1008198. 10.1371/journal.ppat.1008198.
35. Deo, P., Chow, S.H., Han, M.L., Speir, M., Huang, C., Schittenhelm, R.B., Dhital, S., Emery, J., Li, J., Kile, B.T., et al. (2020). Mitochondrial dysfunction caused by outer membrane vesicles from Gram-negative bacteria activates intrinsic apoptosis and inflammation. Nat Microbiol *5*, 1418-1427. 10.1038/s41564-020-0773-2.
36. Esoda, C.N., and Kuehn, M.J. (2019). Pseudomonas aeruginosa Leucine Aminopeptidase Influences Early Biofilm Composition and Structure via Vesicle-Associated Antibiofilm Activity. mBio *10*. 10.1128/mBio.02548-19.
37. Broz, P., Pelegrín, P., and Shao, F. (2020). The gasdermins, a protein family executing cell death and inflammation. Nature reviews. Immunology *20*, 143-157. 10.1038/s41577-019-0228-2.
38. Kayagaki, N., Warming, S., Lamkanfi, M., Vande Walle, L., Louie, S., Dong, J., Newton, K., Qu, Y., Liu, J., Heldens, S., et al. (2011). Non-canonical inflammasome activation targets caspase-11. Nature *479*, 117-121. 10.1038/nature10558.
39. Shi, X., Sun, Q., Hou, Y., Zeng, H., Cao, Y., Dong, M., Ding, J., and Shao, F. (2023). Recognition and maturation of IL-18 by caspase-4 noncanonical inflammasome. Nature *624*, 442-450. 10.1038/s41586-023-06742-w.
40. Wang, K., Sun, Q., Zhong, X., Zeng, M., Zeng, H., Shi, X., Li, Z., Wang, Y., Zhao, Q., Shao, F., and Ding, J. (2020). Structural Mechanism for GSDMD Targeting by Autoprocessed Caspases in Pyroptosis. Cell *180*, 941-955.e920. 10.1016/j.cell.2020.02.002.
41. Zuber, M.X., Strittmatter, S.M., and Fishman, M.C. (1989). A membrane-targeting signal in the amino terminus of the neuronal protein GAP-43. Nature *341*, 345-348. 10.1038/341345a0.
42. Deng, M., Tang, Y., Li, W., Wang, X., Zhang, R., Zhang, X., Zhao, X., Liu, J., Tang, C., Liu, Z., et al. (2018). The Endotoxin Delivery Protein HMGB1 Mediates Caspase-11-Dependent Lethality in Sepsis. Immunity *49*, 740-753.e747. 10.1016/j.immuni.2018.08.016.
43. Vanaja, S.K., Russo, A.J., Behl, B., Banerjee, I., Yankova, M., Deshmukh, S.D., and Rathinam, V.A.K. (2016). Bacterial Outer Membrane Vesicles Mediate Cytosolic Localization of LPS and Caspase-11 Activation. Cell *165*, 1106-1119. 10.1016/j.cell.2016.04.015.
44. Ashida, H., Kim, M., and Sasakawa, C. (2014). Exploitation of the host ubiquitin system by human bacterial pathogens. Nature reviews. Microbiology *12*, 399-413.

10.1038/nrmicro3259.

45. Li, Z., Liu, W., Fu, J., Cheng, S., Xu, Y., Wang, Z., Liu, X., Shi, X., Liu, Y., Qi, X., et al. (2021). Shigella evades pyroptosis by arginine ADP-riboxanation of caspase-11. Nature *599*, 290-295. 10.1038/s41586-021-04020-1.

Figure legends

Figure 1. *P. aeruginosa* infection suppresses NLRP3 inflammasome. (A–E) Wild-type BMDM cells were primed overnight with 1 μg/ml Pam3CSK4 and incubated with *E. coli* or *P. aeruginosa* (ΔRetS PAO1) at an MOI of 30 and 20 μg/ml OMVs for 2 h. Cells were then supplemented with fresh medium containing 100 μg/ml Gentamycin. Cells were lysed and immunoblotted as indicated 16 h post infection (A). Band intensities of cleaved caspase-11 (top) and GSDMD (bottom) were quantified and compared to that of β-actin (B). Cell culture supernatants were collected for an ELISA assay to determine the secreted IL-1β protein levels 16 h post infection (C). Cytotoxicity was determined by LDH release assay in cell culture supernatants 16 h post infection (D). Cell viability was determined by an ATP quantification assay in cell pellets 16 h post infection (E). (F) Wild-type BMDM cells were primed overnight with 1 μg/ml Pam3CSK4 and incubated with *E. coli* or ΔRetS PAO1 at an MOI of 30 and 20 μg/ml OMVs for 2 h. Cells were then supplemented with fresh medium containing 100 μg/ml Gentamycin. Cells were subjected to cellular component fractionation and immunoblotted as indicated 16 h post infection. (G–J) *Aim2*$^{-/-}$ BMDM cells were primed overnight with 1 μg/ml Pam3CSK4, followed by transfection of 2 μg/ml LPS and 2 μg/ml extracted BMDM mitochondrial DNA using DOTAP with or without the incubation of ΔRetS PAO1 at an MOI of 30 for 2 h. Cells were then supplemented with fresh medium containing 100 μg/ml Gentamycin. Cells were lysed and immunoblotted 16 h post infection (G). Cell culture supernatants were collected for an ELISA assay to determine the secreted IL-1β protein levels 16 h post infection (H). Cytotoxicity was determined by LDH release assay in cell culture supernatants 16 h post infection (I). Cell viability was determined by an ATP quantification assay in cell pellets 16 h post infection (J). (K–N) *Casp11*$^{-/-}$;*Aim2*$^{-/-}$ BMDM cells were primed overnight with 1 μg/ml Pam3CSK4, followed by transfection of 2 μg/ml LPS and 2 μg/ml extracted BMDM mitochondrial DNA using DOTAP with or without the incubation of ΔRetS PAO1 at an MOI of 30 for 2 h. Cells were then supplemented with fresh medium containing 100 μg/ml Gentamycin. Cells were lysed and immunoblotted 16 h post infection (K). Cell culture supernatants were collected for an ELISA assay to determine the secreted IL-1β protein levels 16 h post infection (L). Cytotoxicity was determined by LDH release assay in cell

culture supernatants 16 h post infection (M). Cell viability was determined by an ATP quantification assay in cell pellets 16 h post infection (N). Data were shown as means±SD. Experiments were repeated three times with similar results.

Figure 2. *P. aeruginosa* VgrG2b is cleaved by caspase-11. (A) Screening strategy for identifying caspase-11 substrates in *P. aeruginosa*. Briefly, *P. aeruginosa* cDNAs were cloned into GFP vectors containing a mitochondrial localization signal. RFP vectors with a mitochondrial localization signal were used as transfection controls. HEK293T cells were co-transfected with these vectors and caspase-11. Cells losing GFP signals on mitochondria were sequenced. (B, C) Plasmids encoding VgrG2b and mouse caspase-11 p22/p10 (B) or human caspase-4 p22/p10 (C) were co-transfected into HEK293T cells for 24 h, followed by immunoblotting with antibodies against the indicated proteins. (D) Wild-type BMDM cells were primed overnight with 1 μg/ml Pam3CSK4 and incubated with ΔRetS PAO1 or VgrG2b-Myc knockin ΔRetS PAO1 at an MOI of 30 and 20 μg/ml OMVs for 2 h. Cells were then supplemented with fresh medium containing 100 μg/ml Gentamycin. Cells were lysed and immunoblotted as indicated 16 h post infection. (E) Wild-type BMDM cells were primed overnight with 1 μg/ml Pam3CSK4 and incubated with VgrG2b-Myc knockin ΔRetS PAO1 at an MOI of 30 and 20 μg/ml OMVs for 2 h. Cells were then supplemented with fresh medium containing 100 μg/ml Gentamycin. Cells were fixed and stained with antibodies against Myc or caspase-11 16 h post infection. Nucleus was stained with DAPI. Scale bar, 5 μm. (F) *Casp11*$^{+/+}$ and *Casp11*$^{-/-}$ BMDM cells were primed overnight with 1 μg/ml Pam3CSK4, followed by transfection of 2 μg/ml LPS using DOTAP with or without the incubation of VgrG2b-Myc knockin ΔRetS PAO1 at an MOI of 30 for 2 h. Cells were then supplemented with fresh medium containing 100 μg/ml Gentamycin. Cells were lysed and immunoblotted 16 h post infection. (G) *Casp11*$^{-/-}$ BMDM cells were infected with lentiviruses encoding a control vector of caspase-11. Cells were primed overnight with 1 μg/ml Pam3CSK4, followed by transfection of 2 μg/ml LPS using DOTAP with or without the incubation of VgrG2b-Myc knockin ΔRetS PAO1 at an MOI of 30 for 2 h. Cells were then supplemented with fresh medium containing 100 μg/ml Gentamycin. Cells were lysed and immunoblotted as indicated 16 h post infection. (H) *Casp11*$^{-/-}$ BMDM cells

were infected with lentiviruses encoding wild-type or mutant caspase-11. Cells were primed overnight with 1 μg/ml Pam3CSK4, followed by transfection of 2 μg/ml LPS using DOTAP with or without the incubation of VgrG2b-Myc knockin ΔRetS PAO1 at an MOI of 30 for 2 h. Cells were then supplemented with fresh medium containing 100 μg/ml Gentamycin. Cells were lysed and immunoblotted as indicated 16 h post infection. (I) Human macrophages were primed overnight with 1 μg/ml Pam3CSK4, followed by transfection of 2 μg/ml LPS using DOTAP with or without the incubation of VgrG2b-Myc knockin ΔRetS PAO1 at an MOI of 30 for 2 h. Cells were then supplemented with fresh medium containing 100 μg/ml Gentamycin. Cells were lysed and immunoblotted as indicated 16 h post infection. (J–M) Wild-type BMDM cells were primed overnight with 1 μg/ml Pam3CSK4, followed by incubation of VgrG2b-Myc knockin (KI) or knockout (KO) ΔRetS PAO1 at an MOI of 30 and 20 μg/ml OMVs for 2 h. Cells were then supplemented with fresh medium containing 100 μg/ml Gentamycin. Cells were lysed and immunoblotted as indicated 16 h post infection (J). Cell culture supernatants were collected for an ELISA assay to determine the secreted IL-1β protein levels 16 h post infection (K). Cytotoxicity was determined by LDH release assay in cell culture supernatants 16 h post infection (L). Cell viability was determined by an ATP quantification assay in cell pellets 16 h post infection (M). Data were shown as means±SD. Experiments were repeated three times with similar results.

Figure 3. Caspase-11 cleaves VgrG2b at D883. (A) Plasmids encoding VgrG2b and mutant caspase-11 p22/p10 were co-transfected into HEK293T cells for 24 h, followed by immunoprecipitation with a control IgG or antibody against Myc. Precipitates were immunoblotted as indicated. (B) Plasmids encoding caspase-11 p22/p10 and VgrG2b mutants were co-transfected into HEK293T cells for 24 h, followed by immunoblotting with antibodies against the indicated proteins. (C) Plasmids encoding caspase-4 p22/p10 and VgrG2b variants were co-transfected into HEK293T cells for 24 h, followed by immunoblotting with antibodies against the indicated proteins. (D) Plasmids encoding VgrG2a-N-VgrG2b-C chimera and caspase-11 p22/p10 were co-transfected into

HEK293T cells for 24 h, followed by immunoblotting with antibodies against the indicated proteins. (E) Plasmids encoding VgrG2b C-terminus and mutant caspase-11 p22/p10 were co-transfected into HEK293T cells for 24 h, followed by immunoprecipitation with a control IgG or antibody against Myc. Precipitates were immunoblotted as indicated. (F) Recombinant VgrG2b were incubated with caspase-11 p22/p10 for 4 h, followed by immunoblotting with antibodies against the indicated proteins. (G) Wild-type BMDM cells were primed overnight with 1 μg/ml Pam3CSK4, followed by transfection of 2 μg/ml LPS using DOTAP with or without the incubation of VgrG2b wild-type (KI) or mutant (D883A) knockin ΔRetS PAO1 at an MOI of 30 for 2 h. Cells were then supplemented with fresh medium containing 100 μg/ml Gentamycin. Cells were lysed and immunoblotted 16 h post infection. (H–L) Wild-type BMDM cells were primed overnight with 1 μg/ml Pam3CSK4, followed by transfection of 2 μg/ml LPS using DOTAP with or without the incubation of VgrG2b wild-type (KI) or mutant (D883A) knockin ΔRetS PAO1 at an MOI of 30 for 2 h. Cells were then supplemented with fresh medium containing 100 μg/ml Gentamycin. Cells were lysed and immunoblotted as indicated 16 h post infection (H). Band intensities of cleaved caspase-11 (top) and GSDMD (bottom) were quantified and compared to that of β-actin (I). Cell culture supernatants were collected for an ELISA assay to determine the secreted IL-1β protein levels 16 h post infection (J). Cytotoxicity was determined by LDH release assay in cell culture supernatants 16 h post infection (K). Cell viability was determined by an ATP quantification assay in cell pellets 16 h post infection (L). Data were shown as means±SD. Experiments were repeated three times with similar results.

Figure 4. VgrG2b C-terminus interacts with NLRP3. (A) Yeast two-hybrid screening was performed using VgrG2b C-terminus as bait and a mouse bone marrow cDNA library was screened. The interaction strength between bait and preys were visualized by X-α-gal assays. (B, C) Plasmids encoding VgrG2b C-terminus (B) or full-length (C) and NLRP3 were co-transfected into HEK293T cells for 24 h, followed by immunoprecipitation with a control IgG or antibody against Myc. Precipitates were immunoblotted as indicated. (D) VgrG2b C-terminus proteins were introduced into BMDM cells with the help of

867 cell-penetrating peptides (CPP) for 6 h. Cells were lysed and immunoprecipitated with a
868 control IgG or antibody against Myc. Precipitates were immunoblotted as indicated. (E)
869 BMDM cells were primed overnight with 1 μg/ml Pam3CSK4, followed by transfection of 2
870 μg/ml LPS using DOTAP with the incubation of VgrG2b knockin (KI) ΔRetS PAO1 at an
871 MOI of 30 for 2 h. Cells were then supplemented with fresh medium containing 100 μg/ml
872 Gentamycin. Cells were lysed and immunoprecipitated with a control IgG or antibody
873 against NLRP3 16 h post infection. Precipitates were immunoblotted as indicated. (F)
874 BMDM cells were primed overnight with 1 μg/ml Pam3CSK4, followed by transfection of 2
875 μg/ml LPS using DOTAP with the incubation of VgrG2b knockin (KI) ΔRetS PAO1 at an
876 MOI of 30 for 2 h. Cells were then supplemented with fresh medium containing 100 μg/ml
877 Gentamycin. Cells were fixed and stained with antibodies against Myc and NLRP3 16 h
878 post infection. Nucleus was stained with DAPI. Scale bar, 5 μm. (G) Scheme for NLRP3
879 truncations. (H, I) Plasmids encoding VgrG2b C-terminus and NLRP3 truncations were
880 co-transfected into HEK293T cells for 24 h, followed by immunoprecipitation with a control
881 IgG or antibody against FLAG. Precipitates were immunoblotted as indicated. (J)
882 *Casp11*$^{+/+}$ and *Casp11*$^{-/-}$ BMDM cells were primed overnight with 1 μg/ml Pam3CSK4,
883 followed by transfection of 2 μg/ml LPS using DOTAP with the incubation of VgrG2b-Myc
884 knockin (KI) ΔRetS PAO1 at an MOI of 30 for 2 h. Cells were then supplemented with
885 fresh medium containing 100 μg/ml Gentamycin. Cells were lysed and
886 immunoprecipitated with a control IgG or antibody against NLRP3 16 h post infection.
887 Precipitates were immunoblotted as indicated. Data were shown as means±SD.
888 Experiments were repeated three times with similar results.
889
890 **Figure 5. VgrG2b C-terminus suppresses the NLRP3 inflammasome.** (A) Plasmids
891 encoding VgrG2b C-terminus and the indicated murine proteins were co-transfected into
892 HEK293T cells for 24 h, followed by immunoblotting with antibodies against the indicated
893 proteins. (B) Wild-type BMDM cells were infected with lentiviruses encoding a control
894 vector or VgrG2b C-terminus and primed with 1 μg/ml LPS for 3 h, followed by stimulation
895 of 10 μM nigericin for 30 min, 0.5 μM gramicidin for 1 h and 2 mM ATP for 30 min. Cells
896 were lysed and immunoblotted as indicated. (C–G) Wild-type BMDM cells were primed

overnight with 1 μg/ml Pam3CSK4, followed by transfection of 2 μg/ml LPS using DOTAP with or without the transfection of VgrG2b C-terminus proteins using cell-penetrating peptides (CPP) for 2 h. Cells were then supplemented with fresh medium. Cells were lysed and immunoblotted 16 h post transfection (C). Band intensities of cleaved caspase-11 (top) and GSDMD (bottom) were quantified and compared to that of β-actin (D). Cell culture supernatants were collected for an ELISA assay to determine the secreted IL-1β protein levels 16 h post infection (E). Cytotoxicity was determined by LDH release assay in cell culture supernatants 16 h post infection (F). Cell viability was determined by an ATP quantification assay in cell pellets 16 h post infection (G). (H, I) Wild-type BMDM cells were primed overnight with 1 μg/ml Pam3CSK4, followed by transfection of 2 μg/ml LPS using DOTAP with or without the transfection of VgrG2b C-terminus proteins using cell-penetrating peptides (CPP) for 2 h. Cells were then supplemented with fresh medium. Cells were lysed and immunoprecipitated with a control IgG or antibody against NLRP3 16 h post transfection. Precipitates were immunoblotted with antibody against Nur77 (H) or NEK7 (I). (J) Plasmids encoding VgrG2b C-terminus, NEK7 and NLRP3 were co-transfected into HEK293T cells for 24 h, followed by immunoprecipitation with a control IgG or antibody against NLRP3. Precipitates were immunoblotted as indicated. Data were shown as means±SD. Experiments were repeated three times with similar results.

Figure 6. *P. aeruginosa* suppresses NLRP3 inflammasome *in vivo*. (A–E) Wild-type mice were intraperitoneally challenged with poly(I:C) at a dose of 2 mg/kg body weight for 6 h and then intranasally infected with $1x10^9$ cfu of VgrG2b (KI) or mutant (D883A) knockin ΔRetS PAO1, followed by survival calculation at the indicated days (A). Serum protein levels of IL-1β (B), TNF-α (C) and IL-6 (D) were examined through ELISA assays 24 h post infection. Bacterial load was examined in mouse lung tissues 4 days post infection (E). (F–J) Wild-type mice were intraperitoneally challenged with poly(I:C) at a dose of 2 mg/kg body weight for 6 h and then intranasally infected with $1x10^9$ cfu of VgrG2b (KI) or mutant (D883A) knockin ΔRetS PAO1. Bronchoalveolar lavage fluids (BALF) were collected 16 h post infection. Cells were immunoblotted as indicated (F). Cell

viability was also determined by an ATP quantification assay in cell pellets (G). Protein levels of IL-1β (H), TNF-α (I) and IL-6 (J) in BALF supernatants were examined through ELISA assays. (K–O) Wild-type mice were intraperitoneally challenged with poly(I:C) at a dose of 2 mg/kg body weight for 6 h and then intranasally infected with $1x10^9$ cfu of ΔRetS PAO1 and administrated with 20 μg TAT sequence containing VgrG2b C-terminus peptide, followed by survival calculation at the indicated days (K). Serum protein levels of IL-1β (L), TNF-α (M) and IL-6 (N) were examined through ELISA assays 24 h post infection. Bacterial load was examined in mouse lung tissues 4 days post infection (O). Data were shown as means±SD. Experiments were repeated three times with similar results.

Figure 1

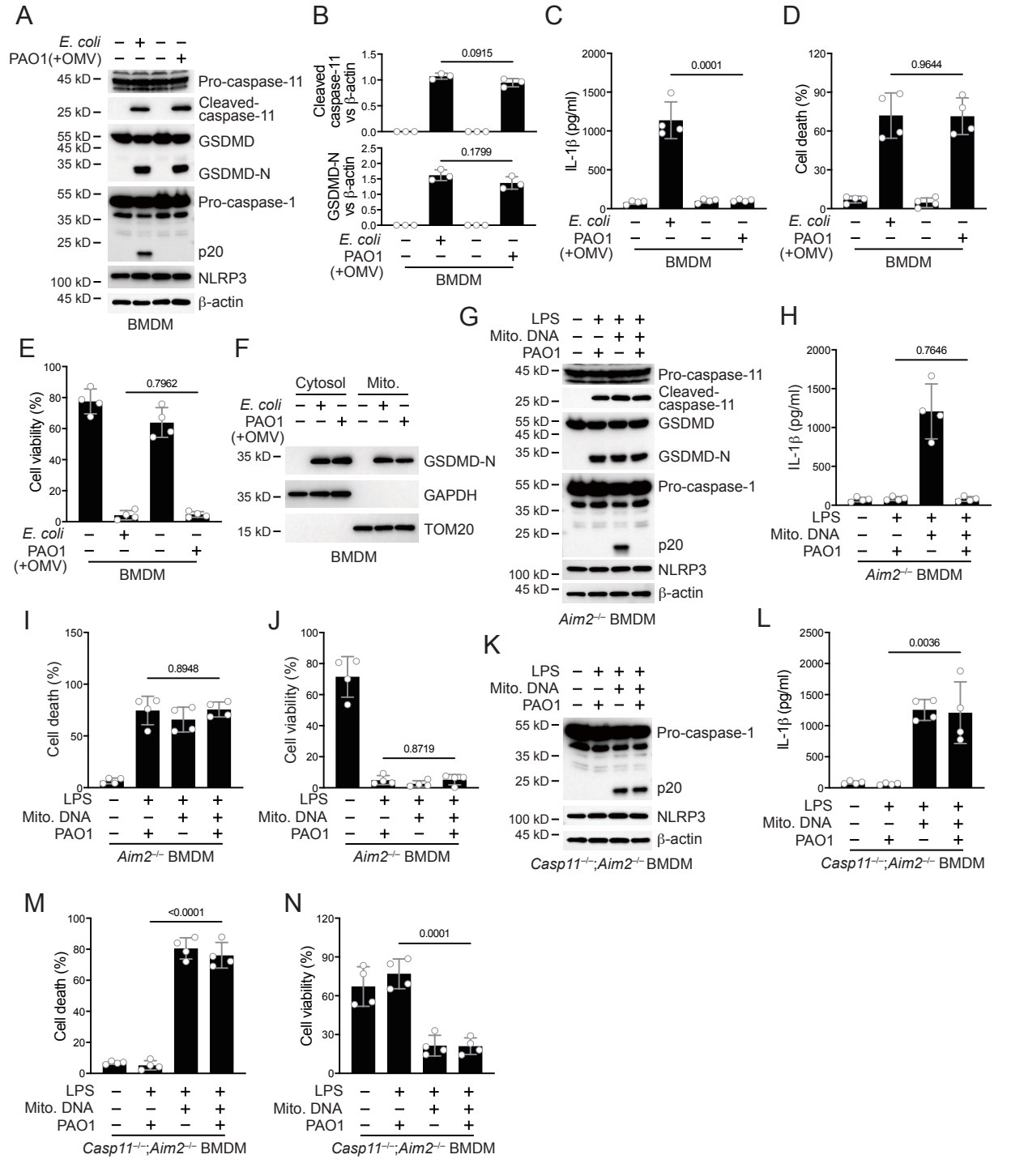
A
E. coli
PAO1(+OMV)
45 kD
Pro-caspase-11
25 kD
Cleaved-caspase-11
55 kD
45 kD
GSDMD
35 kD
GSDMD-N
55 kD
Pro-caspase-1
35 kD
25 kD
p20
100 kD
NLRP3
45 kD
β-actin
BMDM
B
Cleaved caspase-11 vs β-actin
0.0915
GSDMD-N vs β-actin
0.1799
E. coli
PAO1 (+OMV)
BMDM
C
IL-1β (pg/ml)
0.0001
E. coli
PAO1 (+OMV)
BMDM
D
Cell death (%)
0.9644
E. coli
PAO1 (+OMV)
BMDM
E
Cell viability (%)
0.7962
E. coli
PAO1 (+OMV)
BMDM
F
Cytosol
Mito.
E. coli
PAO1 (+OMV)
35 kD
GSDMD-N
35 kD
GAPDH
15 kD
TOM20
BMDM
G
LPS
Mito. DNA
PAO1
45 kD
Pro-caspase-11
25 kD
Cleaved-caspase-11
55 kD
45 kD
GSDMD
35 kD
GSDMD-N
55 kD
Pro-caspase-1
35 kD
25 kD
p20
100 kD
NLRP3
45 kD
β-actin
Aim2−/− BMDM
H
IL-1β (pg/ml)
0.7646
LPS
Mito. DNA
PAO1
Aim2−/− BMDM
I
Cell death (%)
0.8948
LPS
Mito. DNA
PAO1
Aim2−/− BMDM
J
Cell viability (%)
0.8719
LPS
Mito. DNA
PAO1
Aim2−/− BMDM
K
LPS
Mito. DNA
PAO1
55 kD
Pro-caspase-1
35 kD
25 kD
p20
100 kD
NLRP3
45 kD
β-actin
Casp11−/−;Aim2−/− BMDM
L
IL-1β (pg/ml)
0.0036
LPS
Mito. DNA
PAO1
Casp11−/−;Aim2−/− BMDM
M
Cell death (%)
<0.0001
LPS
Mito. DNA
PAO1
Casp11−/−;Aim2−/− BMDM
N
Cell viability (%)
0.0001
LPS
Mito. DNA
PAO1
Casp11−/−;Aim2−/− BMDM

Figure 2

A

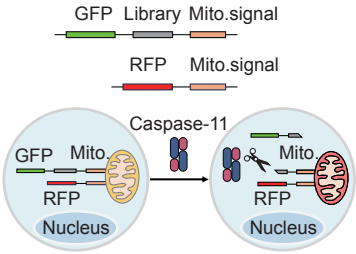

B

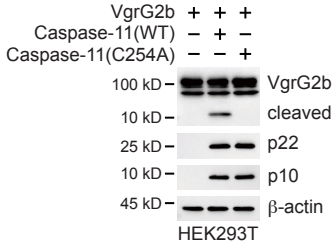

C

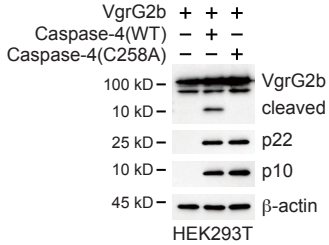

D

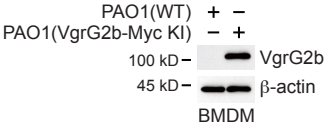

E

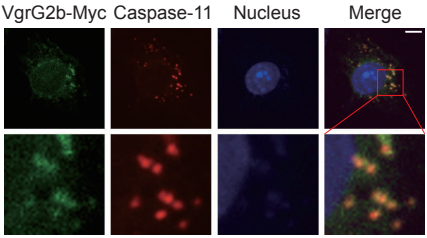

F

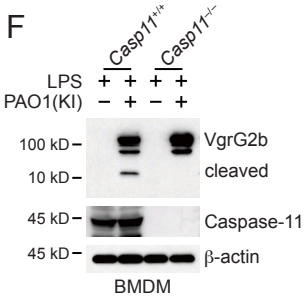

G

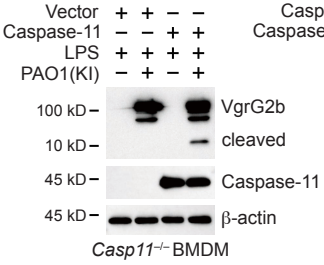

H

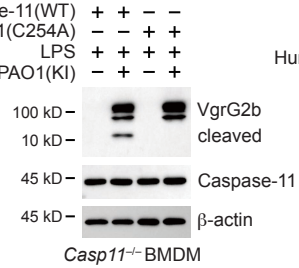

I

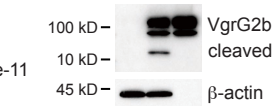

J

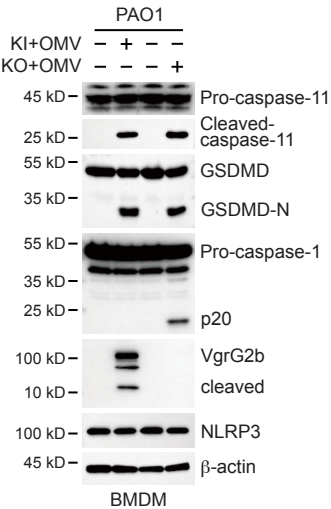

K

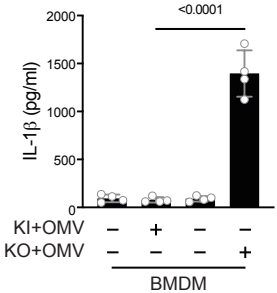

L

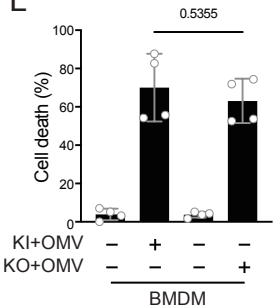

M

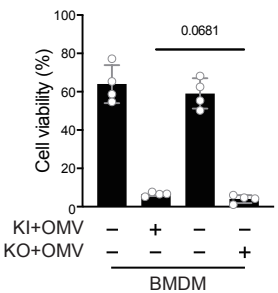

Figure 3

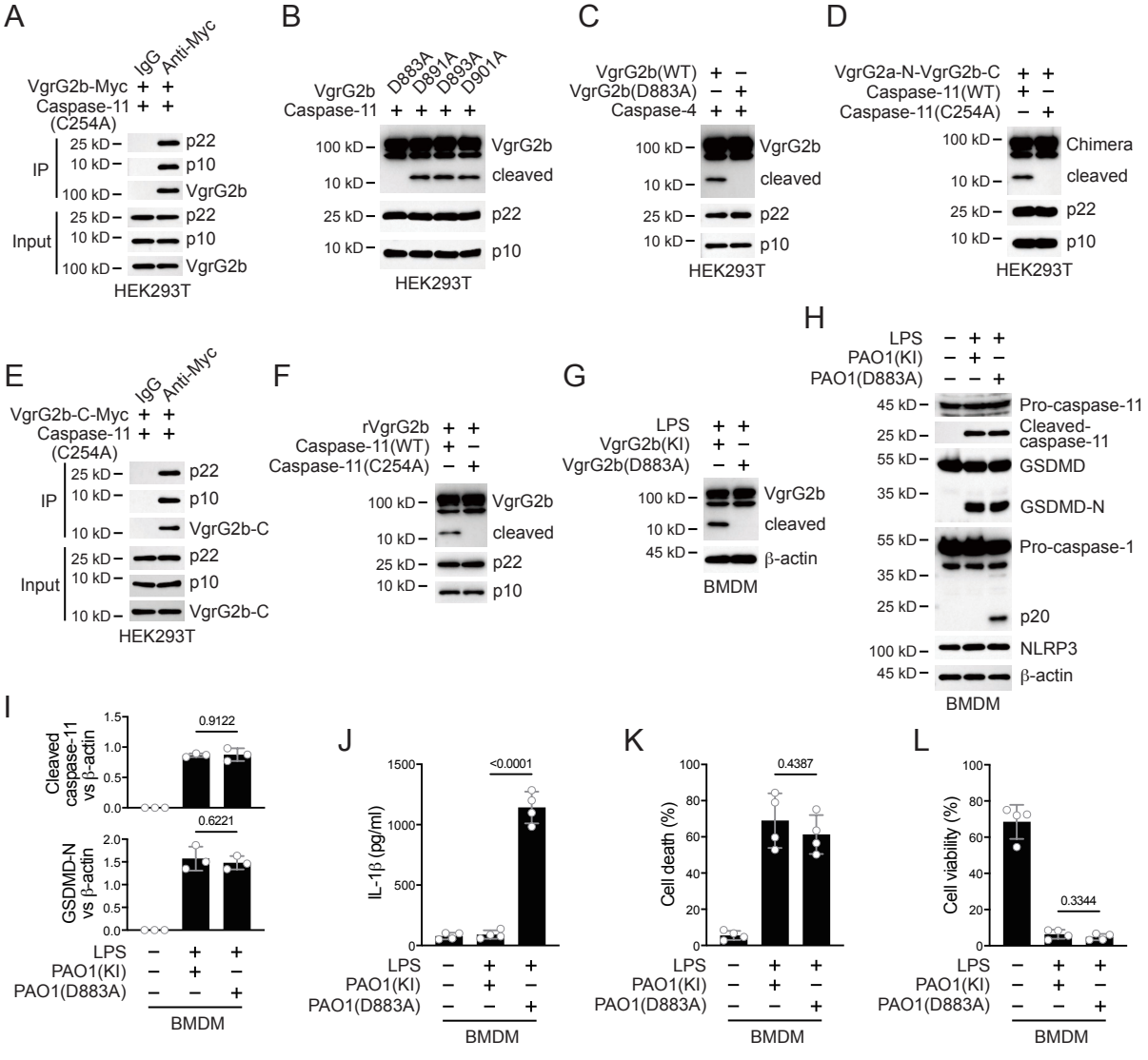
A
IgG
Anti-Myc
VgrG2b-Myc + +
Caspase-11 (C254A) + +
IP
Input
25 kD
10 kD
100 kD
p22
p10
VgrG2b
HEK293T
B
VgrG2b
D883A
D891A
D893A
D901A
Caspase-11 + + + +
100 kD
10 kD
25 kD
VgrG2b
cleaved
p22
p10
HEK293T
C
VgrG2b(WT) + −
VgrG2b(D883A) − +
Caspase-4 + +
100 kD
10 kD
25 kD
VgrG2b
cleaved
p22
p10
HEK293T
D
VgrG2a-N-VgrG2b-C + +
Caspase-11(WT) + −
Caspase-11(C254A) − +
100 kD
10 kD
25 kD
Chimera
cleaved
p22
p10
HEK293T
E
IgG
Anti-Myc
VgrG2b-C-Myc + +
Caspase-11 (C254A) + +
IP
Input
25 kD
10 kD
p22
p10
VgrG2b-C
HEK293T
F
rVgrG2b + +
Caspase-11(WT) + −
Caspase-11(C254A) − +
100 kD
10 kD
25 kD
10 kD
VgrG2b
cleaved
p22
p10
G
LPS + +
VgrG2b(KI) + −
VgrG2b(D883A) − +
100 kD
10 kD
45 kD
VgrG2b
cleaved
β-actin
BMDM
H
LPS − + +
PAO1(KI) − + −
PAO1(D883A) − − +
45 kD
25 kD
55 kD
35 kD
55 kD
35 kD
25 kD
100 kD
45 kD
Pro-caspase-11
Cleaved-caspase-11
GSDMD
GSDMD-N
Pro-caspase-1
p20
NLRP3
β-actin
BMDM
I
Cleaved caspase-11 vs β-actin
0.9122
GSDMD-N vs β-actin
0.6221
LPS − + +
PAO1(KI) − + −
PAO1(D883A) − − +
BMDM
J
IL-1β (pg/ml)
<0.0001
LPS − + +
PAO1(KI) − + −
PAO1(D883A) − − +
BMDM
K
Cell death (%)
0.4387
LPS − + +
PAO1(KI) − + −
PAO1(D883A) − − +
BMDM
L
Cell viability (%)
0.3344
LPS − + +
PAO1(KI) − + −
PAO1(D883A) − − +
BMDM

Figure 4

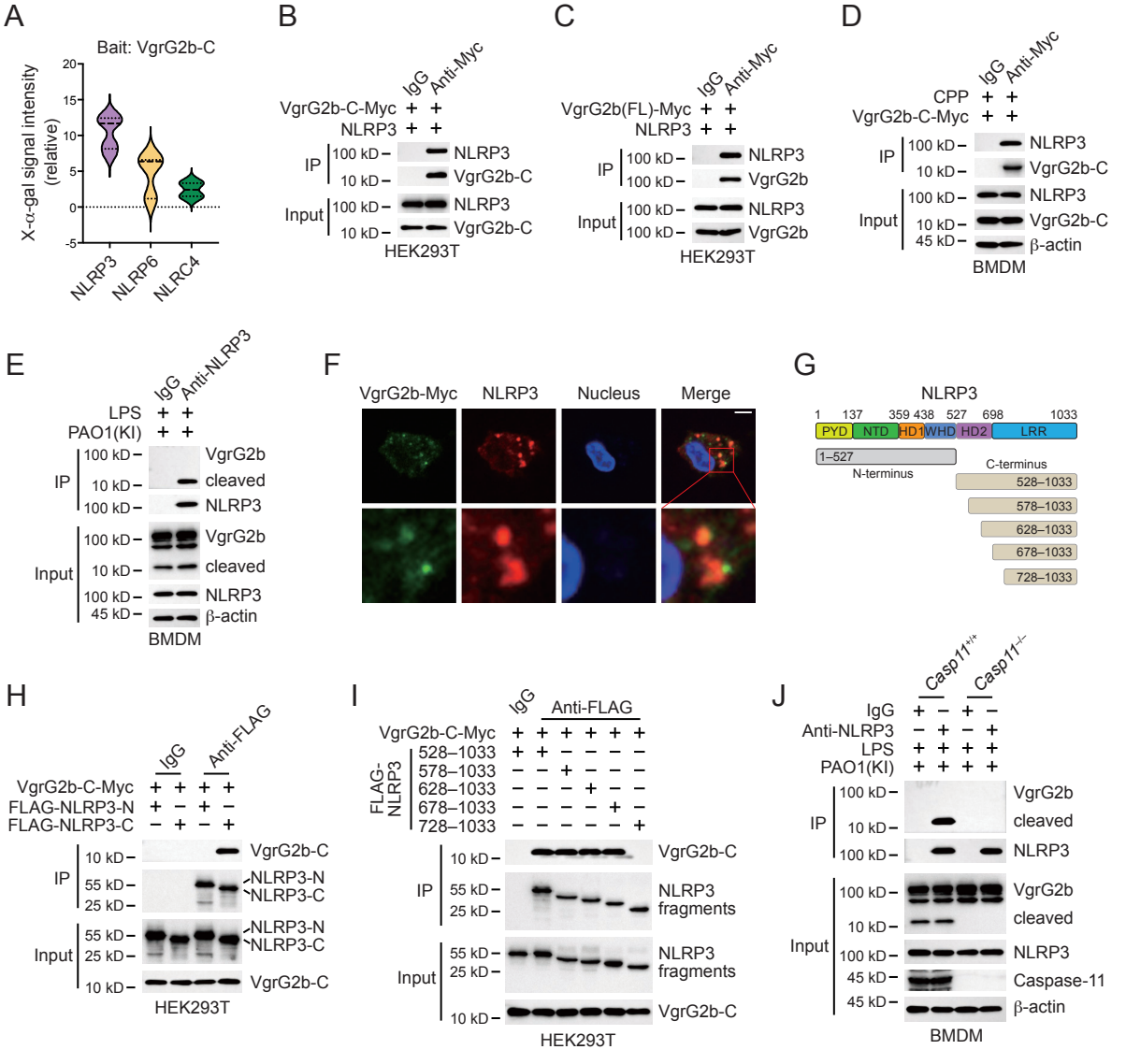
A
Bait: VgrG2b-C
X-α-gal signal intensity (relative)
20
15
10
5
0
-5
NLRP3
NLRP6
NLRC4
B
IgG
Anti-Myc
VgrG2b-C-Myc + +
NLRP3 + +
IP
100 kD
10 kD
NLRP3
VgrG2b-C
Input
100 kD
10 kD
NLRP3
VgrG2b-C
HEK293T
C
IgG
Anti-Myc
VgrG2b(FL)-Myc + +
NLRP3 + +
IP
100 kD
100 kD
NLRP3
VgrG2b
Input
100 kD
100 kD
NLRP3
VgrG2b
HEK293T
D
IgG
Anti-Myc
CPP + +
VgrG2b-C-Myc + +
IP
100 kD
10 kD
NLRP3
VgrG2b-C
Input
100 kD
10 kD
45 kD
NLRP3
VgrG2b-C
β-actin
BMDM
E
IgG
Anti-NLRP3
LPS + +
PAO1(KI) + +
IP
100 kD
10 kD
100 kD
VgrG2b
cleaved
NLRP3
Input
100 kD
10 kD
100 kD
45 kD
VgrG2b
cleaved
NLRP3
β-actin
BMDM
F
VgrG2b-Myc
NLRP3
Nucleus
Merge
G
NLRP3
1
137
359
438
527
698
1033
PYD
NTD
HD1
WHD
HD2
LRR
1–527
N-terminus
C-terminus
528–1033
578–1033
628–1033
678–1033
728–1033
H
IgG
Anti-FLAG
VgrG2b-C-Myc + + + +
FLAG-NLRP3-N + − + −
FLAG-NLRP3-C − + − +
IP
10 kD
55 kD
25 kD
VgrG2b-C
NLRP3-N
NLRP3-C
Input
55 kD
25 kD
10 kD
NLRP3-N
NLRP3-C
VgrG2b-C
HEK293T
I
IgG
Anti-FLAG
VgrG2b-C-Myc + + + + + +
FLAG-NLRP3
528–1033 + + − − − −
578–1033 − − + − − −
628–1033 − − − + − −
678–1033 − − − − + −
728–1033 − − − − − +
IP
10 kD
55 kD
25 kD
VgrG2b-C
NLRP3 fragments
Input
55 kD
25 kD
10 kD
NLRP3 fragments
VgrG2b-C
HEK293T
J
Casp11+/+
Casp11−/−
IgG + − + −
Anti-NLRP3 − + − +
LPS + + + +
PAO1(KI) + + + +
IP
100 kD
10 kD
100 kD
VgrG2b
cleaved
NLRP3
Input
100 kD
10 kD
100 kD
45 kD
45 kD
VgrG2b
cleaved
NLRP3
Caspase-11
β-actin
BMDM

Figure 5

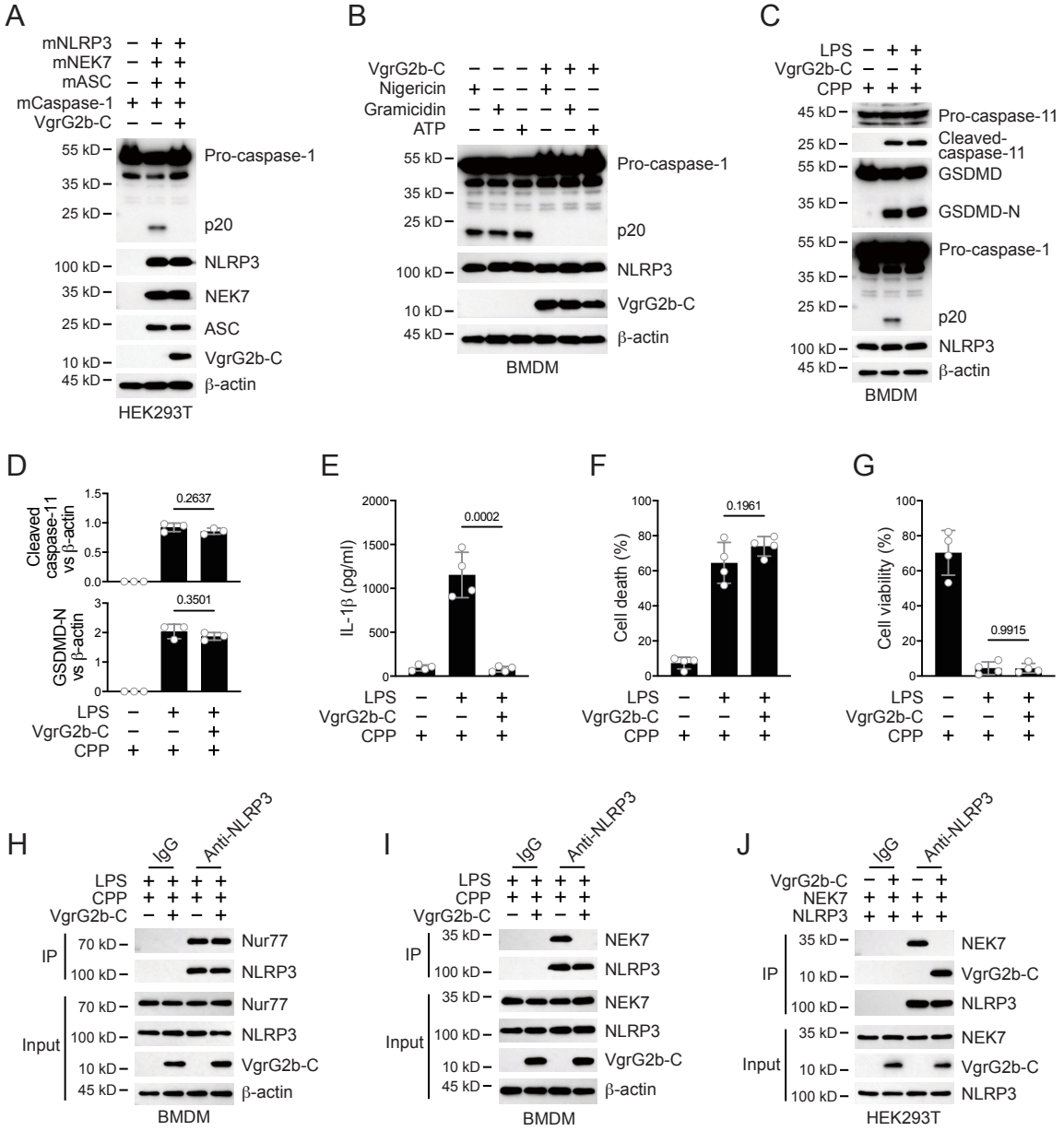
A
mNLRP3 − + +
mNEK7 − + +
mASC − + +
mCaspase-1 + + +
VgrG2b-C − − +
55 kD
35 kD
25 kD
Pro-caspase-1
p20
100 kD
NLRP3
35 kD
NEK7
25 kD
ASC
10 kD
VgrG2b-C
45 kD
β-actin
HEK293T
B
VgrG2b-C − − − + + +
Nigericin + − − + − −
Gramicidin − + − − + −
ATP − − + − − +
55 kD
Pro-caspase-1
35 kD
25 kD
p20
100 kD
NLRP3
10 kD
VgrG2b-C
45 kD
β-actin
BMDM
C
LPS − + +
VgrG2b-C − − +
CPP + + +
45 kD
Pro-caspase-11
25 kD
Cleaved-caspase-11
55 kD
GSDMD
35 kD
GSDMD-N
55 kD
Pro-caspase-1
35 kD
25 kD
p20
100 kD
NLRP3
45 kD
β-actin
BMDM
D
Cleaved caspase-11 vs β-actin
1.5
1.0
0.5
0.0
0.2637
GSDMD-N vs β-actin
3
2
1
0
0.3501
LPS − + +
VgrG2b-C − − +
CPP + + +
E
IL-1β (pg/ml)
2000
1500
1000
500
0
0.0002
LPS − + +
VgrG2b-C − − +
CPP + + +
F
Cell death (%)
100
80
60
40
20
0
0.1961
LPS − + +
VgrG2b-C − − +
CPP + + +
G
Cell viability (%)
100
80
60
40
20
0
0.9915
LPS − + +
VgrG2b-C − − +
CPP + + +
H
IgG
Anti-NLRP3
LPS + + + +
CPP + + + +
VgrG2b-C − + − +
IP
70 kD
Nur77
100 kD
NLRP3
Input
70 kD
Nur77
100 kD
NLRP3
10 kD
VgrG2b-C
45 kD
β-actin
BMDM
I
IgG
Anti-NLRP3
LPS + + + +
CPP + + + +
VgrG2b-C − + − +
IP
35 kD
NEK7
100 kD
NLRP3
Input
35 kD
NEK7
100 kD
NLRP3
10 kD
VgrG2b-C
45 kD
β-actin
BMDM
J
IgG
Anti-NLRP3
VgrG2b-C − + − +
NEK7 + + + +
NLRP3 + + + +
IP
35 kD
NEK7
10 kD
VgrG2b-C
100 kD
NLRP3
Input
35 kD
NEK7
10 kD
VgrG2b-C
100 kD
NLRP3
HEK293T

Figure 6

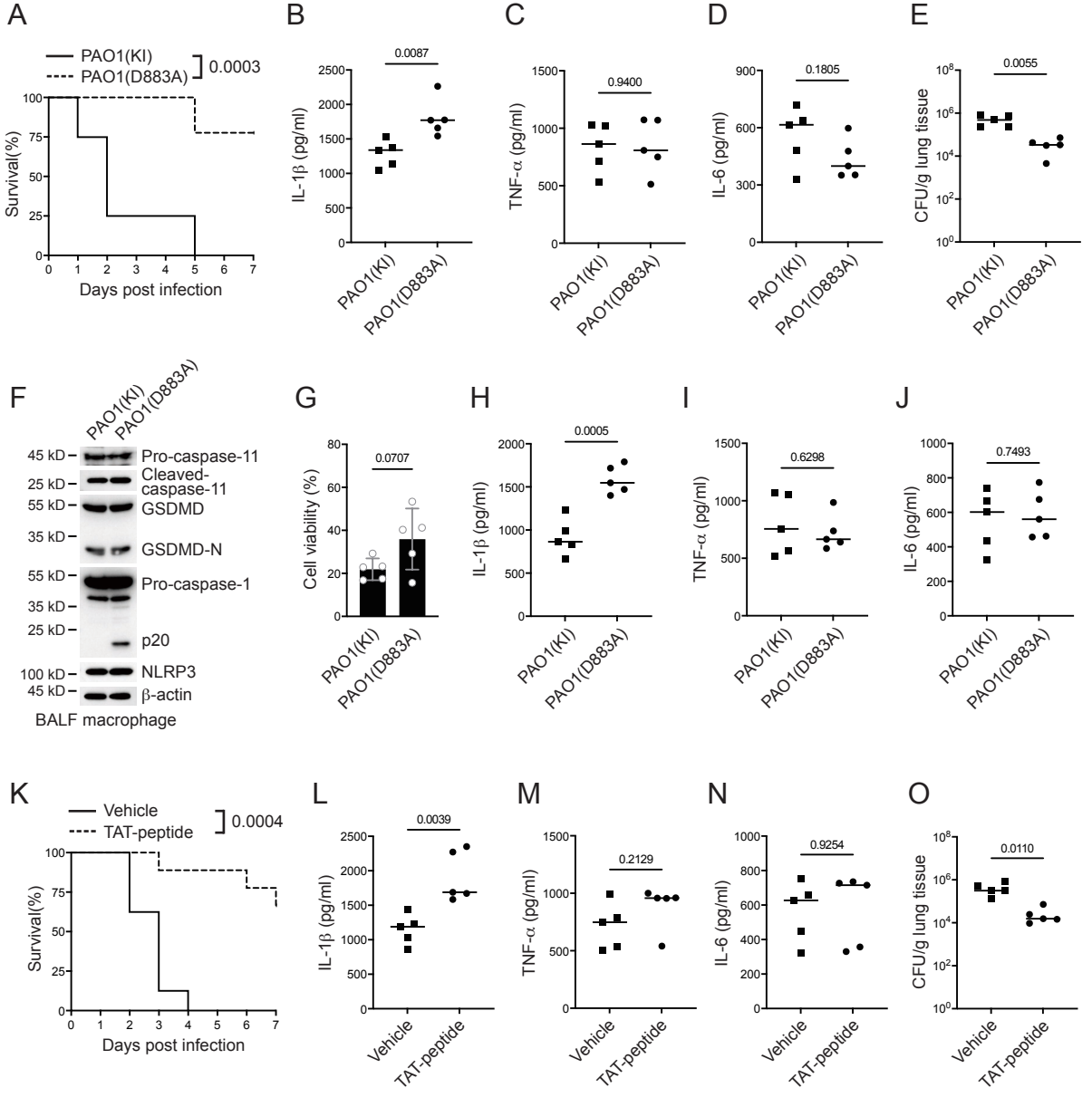
A
PAO1(KI)
PAO1(D883A)
0.0003
Survival(%)
Days post infection
B
0.0087
IL-1β (pg/ml)
PAO1(KI)
PAO1(D883A)
C
0.9400
TNF-α (pg/ml)
D
0.1805
IL-6 (pg/ml)
E
0.0055
CFU/g lung tissue
F
PAO1(KI)
PAO1(D883A)
45 kD
Pro-caspase-11
25 kD
Cleaved-caspase-11
55 kD
GSDMD
35 kD
GSDMD-N
55 kD
Pro-caspase-1
35 kD
25 kD
p20
100 kD
NLRP3
45 kD
β-actin
BALF macrophage
G
0.0707
Cell viability (%)
H
0.0005
I
0.6298
J
0.7493
K
Vehicle
TAT-peptide
0.0004
L
0.0039
M
0.2129
N
0.9254
O
0.0110